

# Neutron and X-ray Diffraction and Spectroscopic Investigations of Intramolecular [C–H...F–C] Contacts in Post-Metallocene Polyolefin Catalysts: Modeling Weak Attractive Polymer–Ligand Interactions

Michael C. W. Chan,<sup>\*,[a]</sup> Steven C. F. Kui,<sup>[b]</sup> Jacqueline M. Cole,<sup>\*,[c]</sup> Garry J. McIntyre,<sup>[d]</sup> Shigekazu Matsui,<sup>[e]</sup> Nianyong Zhu,<sup>[b]</sup> and Ka-Ho Tam<sup>[b]</sup>

**Abstract:** A family of Group 4 post-metallocene catalysts, supported by fluorine-functionalized tridentate ligands with the fluorine substituent in the locality of the metal center, is described. For the first time, the contentious C–H...F–C interaction has been characterized by a neutron diffraction study, which has allowed the position of the hydrogen atoms to be accurately determined. The nature of the weak intramolecular C–H...F–C contacts in these complexes in solution and the solid state was probed by using multinuclear NMR spectroscopy in tandem with

neutron and X-ray crystallography. Evidence is presented to demonstrate that the spectroscopic C–H...F–C coupling occurs “through-space” rather than “through-bond” or by M...F coordination. The titanium catalysts exhibit excellent activities and high co-monomer incorporation in olefin polymerization. The observed intramolecular

C–H...F–C interactions are important with regards to potential applications in polyolefin catalysis because they substantiate the proposed *ortho*-F...H( $\beta$ ) ligand–(polymer chain) contacts derived from DFT calculations for the remarkable fluorinated phenoxyimine Group 4 catalysts. Compared with agostic and co-catalyst...metal contacts, weak attractive noncovalent interactions between a polymer chain and a judiciously designed “active” ligand is a new concept in polyolefin catalysis.

**Keywords:** fluorinated ligands • hydrogen bonds • neutron diffraction • noncovalent interactions • post-metallocenes

## Introduction

The consideration of weak transient attractive interactions has been instrumental in the development of metal-catalyzed olefin polymerization reactions. The existence of agos-

tic interactions between the  $\alpha$ -(plus  $\beta$ - and  $\gamma$ -)hydrogen atoms of the polymer chain and the metal center during the polymerization process, which influences the rate of olefin insertion and migration, is well-established.<sup>[1,2]</sup> The weak metal-coordinating capabilities (C–F...M) of putative “non-


[a] Dr. M. C. W. Chan  
Department of Biology and Chemistry  
City University of Hong Kong  
Tat Chee Avenue, Kowloon, Hong Kong (China)  
Fax: (+852) 2788-7406  
E-mail: mcwchan@cityu.edu.hk

[b] S. C. F. Kui, Dr. N. Zhu, K.-H. Tam  
Department of Chemistry and HKU-CAS Joint Laboratory on New Materials  
The University of Hong Kong, Pokfulam Road, Hong Kong (China)

[c] Dr. J. M. Cole  
Department of Chemistry, University of Cambridge  
Lensfield Road, Cambridge, CB2 1EW (UK)  
Office Mailing Address: St. Catharine's College  
Cambridge, CB2 1RL (UK)  
Fax: (+44) 1223-338-340  
E-mail: jmc61@cam.ac.uk

[d] Dr. G. J. McIntyre  
Institut Laue-Langevin, B.P. 156, 38042 Grenoble Cedex 9 (France)

[e] Dr. S. Matsui  
R&D Center, Mitsui Chemicals, Inc., 580-32 Nagaura  
Sodegaura, Chiba 299-0265 (Japan)

 Supporting information (experimental details and characterization data, perspective views of **4**, **7**, and **12**, NMR spectra of **10** showing effects of <sup>19</sup>F decoupling, details of DFT calculations, results from a CSD search for neutron structures containing C–H and F–C bonds) for this article is available on the WWW under <http://www.chemeur-j.org/> or from the author.

interacting" perfluorinated anion co-catalysts (for example,  $B(C_6F_5)_3$ ) have become apparent and can cause catalyst deactivation,<sup>[3]</sup> but these initiators have also been utilized to stabilize extremely electron-deficient and coordinatively unsaturated catalytic centers, especially when integrated into the spectator ligand.<sup>[4]</sup> This approach is conceptually related to the development of polydentate "hemilabile" ligands<sup>[5]</sup> in olefin polymerization and other catalytic processes,<sup>[6]</sup> whereby a substitutionally labile moiety can be displaced from and yet remain available for recoordination to the reactive metal species in a reversible manner. Conversely, repulsive nonbonding interactions (and steric effects) between bulky ancillary ligands and the incoming prochiral olefin form the basis for controlling the stereoselectivity of metallocene-catalyzed  $\alpha$ -olefin polymerization reactions.<sup>[2c,7]</sup>

Weak noncovalent interactions between a functionalized ligand and the polymer chain offer intriguing possibilities, but there is no precedent for their exploration. In contrast to steric repulsion, fragile attractive forces are inherently tunable in a rational fashion. Like agostic and co-catalyst-metal contacts, the development of ligand-polymer interactions is feasible only if the interaction is dynamic and the polymerization process (e.g. chain propagation) is not interrupted. Significantly, a remarkably active and versatile class of fluorinated phenoxyimine Group 4 polyolefin catalysts was recently described. The abilities of these titanium "FI" catalysts, pioneered by Fujita and co-workers,<sup>[8]</sup> to mediate living polyethylene formation at high temperatures (up to 70°C) and syndiotactic living propylene polymerization with exceedingly rare 2,1-insertions have been reported, while the robust living nature of these catalysts has been exploited for the fabrication of new multiblock copolymers and chain-end functionalized polyolefin materials. Coates and co-workers observed exclusive 2,1-regiochemistry for propylene insertion in homo-, co-, and cyclopolymerization reactions using these catalysts, and very recently achieved isotacticity and living behavior for propylene polymerization using fluorine-rich phenoxyketimine titanium catalysts.<sup>[9,10]</sup> Theoretical investigations aimed at rationalizing these impressive results, and in particular the unusual stereoselectivity, have been carried out.<sup>[11]</sup>

To elucidate the role the fluorine groups have in living polymerization reactions, Fujita and co-workers performed computational analysis on several active species derived from these catalysts.<sup>[8e-g]</sup> The DFT calculations indicated the existence of a weak C-H...F-C interaction between the fluorine atom *ortho* to the imine nitrogen and a  $\beta$ -hydrogen atom of the polymer chain, which would inhibit  $\beta$ -hydrogen transfer to the metal and/or a reacting monomer, resulting in chain termination. This clearly emphasizes the potential importance of noncovalent attractive ligand-polymer interactions for stabilizing  $\beta$ -hydrogen atoms and achieving living polymerization processes. Furthermore, it is envisaged that such weak contacts may allow manipulation of the reactivity at the polymer chain and offer new opportunities to create novel polymeric microstructures and materials.

The C-H...F-C interaction is one of the weakest hydrogen bonds to be scrutinized. Indeed, the existence, nature, and relevance (in a crystallographic context) of this interaction are all highly contentious issues that have been discussed in numerous critical reviews over the last decade.<sup>[12]</sup> Nevertheless, the body of structural evidence from X-ray crystallography in support of C-H...F-C contacts, with H...F separations less than the sum of their van der Waals radii (2.5–2.7 Å),<sup>[13]</sup> plus their impact in the realm of crystal engineering, is conspicuous.<sup>[14]</sup> Advanced rotational spectroscopic techniques have been employed to probe the weak C-H...F-C bridges between bimolecular fluoromethane species in the gas phase<sup>[15]</sup> and these investigations have been complemented by systematic theoretical calculations.<sup>[16]</sup> In materials science, C-H...F-C contacts have been invoked to explain the solid-state organization and physical and molecular characteristics of fluorinated conjugated organic materials with emerging applications in optoelectronics.<sup>[17]</sup> With regards to biological recognition, the exploitation of fluorinated substituents and the accompanying C-H...F-C interactions to enhance the affinity and selectivity at enzyme active sites and in RNA and DNA bases has recently been advocated,<sup>[18]</sup> while close C-H...F-C contacts in the crystal structures of fluorine-rich molecular sensors and receptors have also been observed.<sup>[19]</sup>

A key focus of our studies in post-metallocene polyolefin catalyst design is the development of nonsymmetric tridentate ancillary ligands.<sup>[20]</sup> We began to explore the possibility of using aryl  $\sigma$ -carbanion moieties as a chelating group since the resultant M-C(sp<sup>2</sup>) bond should be relatively covalent (affording a highly electrophilic catalytic center) and its inertness is, crucially, expected to be greater than those of its aliphatic M-C(sp<sup>3</sup>) counterparts. Our preliminary report<sup>[21]</sup> described the first direct spectroscopic and X-ray crystallographic evidence for the presence of weak C-H...F-C interactions in fluorinated Group 4 polyolefin catalysts, which are reminiscent of the *ortho*-F...H( $\beta$ ) contacts proposed by Fujita and co-workers.<sup>[8]</sup> The use of X-ray crystal structures to validate hydrogen-bonding interactions is nevertheless questionable because the positions of hydrogen atoms cannot be determined accurately; this can only be achieved by employing neutron crystallography. We now present the neutron structure of a fluorinated zirconium catalyst and, to the best of our knowledge, this is the first time that the controversial C-H...F-C interaction has been characterized by neutron diffraction.

Herein we describe the synthesis of a series of fluorine-substituted Group 4 catalysts and their characterization by a variety of NMR spectroscopic and X-ray and neutron crystallographic techniques. The abilities of these complexes to mediate homo- and copolymerization processes in conjunction with different co-catalysts have been evaluated and of particular interest are the high activities and excellent degrees of co-monomer incorporation observed. It is envisaged that a greater insight into the nature of the C-H...F-C contacts apparent in these catalysts can be derived and a possible correlation between the magnitude of the spectroscopic

C–H...F–C coupling and the associated structural parameters is examined.

## Results and Discussion

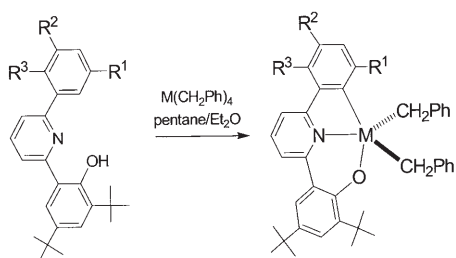
**Synthesis of Group 4 complexes bearing a fluorinated aryl  $\sigma$ -carbanion moiety:** Tremendous progress has been achieved recently in the design of new-generation non-metallocene olefin polymerization catalysts.<sup>[22]</sup> In the context of this work, it is notable that non-cyclopentadienyl carbon-based anionic ligand sets are rarely investigated and the resultant complexes typically exhibit poor-to-moderate catalytic performances.<sup>[23]</sup> With respect to aromatic  $\sigma$ -carbanions, zirconium complexes with bis( $\sigma$ -aryl)amine dianionic tridentate ligands have been reported as catalysts for propylene polymerization, but low activities were observed.<sup>[24]</sup> Furthermore, descriptions of the use of fluorine-rich supporting ligands in post-metallocene polyolefin catalysts are sparse in the literature.<sup>[25]</sup> To model the weak C–H...F–C contacts proposed by Fujita and co-workers,<sup>[8]</sup> our synthetic approach targeted the generation of complexes containing fluorine-functionalized ancillary ligands. Specifically, we endeavored to position a fluorinated substituent in the vicinity of the metal (e.g. *ortho* to the C(carbanion) atom; see below) so that weak noncovalent interactions with metal-bound alkyl/polymer chains become feasible.

A versatile procedure for the preparation of nonsymmetric 2-(2'-hydroxyphenyl)-6-arylpipridine substrates has been devised,<sup>[20]</sup> which in essence entails the sequential coupling of two substituted acetophenone molecules. Metalation of these substrates, which possess acidic protons, proceeds upon reaction with the basic  $[M(\text{CH}_2\text{Ph})_4]$  ( $M = \text{Zr}, \text{Ti}$ ) or  $[\text{Zr}(\text{CH}_2\text{Ph})_2\text{Cl}_2(\text{OEt}_2)_2]$  precursors and is accompanied by the elimination of toluene to afford complexes **1–12** as yellow-orange (Zr) to red (Ti) crystalline solids (Scheme 1). For **7** and **8**, the presence of THF as a donor facilitates complex isolation. The cyclometalation process readily takes place at 25 °C and is observed to be highly regioselective. Hence, for substrates in which two potential cyclometalation sites exist (i.e.  $R^1 \neq R^2$ ,  $R^3 = \text{H}$ ), only the pictured compound (**4**, **6**, **8**, and **12**; in which  $R^1$  is less sterically demanding than  $R^2$ ) has been isolated or detected by  $^1\text{H}$  NMR spectroscopy. Generation of **2** and **10** by C–H activation is clearly more

favorable thermodynamically than C–F activation. The derivatives are thus designed with a  $\text{CF}_3$  (**1**, **2**, **9**, and **10**) or F substituent (**6**, **8**, and **12**) at the *ortho* ( $R^1$ ) position of the aryl  $\sigma$ -carbanion moiety, which is in close proximity to, *but not interacting with*, the metal core. In place of the fluorinated group, complexes bearing a methyl substituent (**3** and **11**) or only a hydrogen atom (**4**, **5**, and **7**) at  $R^1$  have been prepared for comparison purposes. We note that attempts to synthesize titanium and zirconium derivatives with *tert*-butyl groups as the  $R^1$  and  $R^2$  substituents yielded intractable mixtures, characterization of which ( $^1\text{H}$  NMR) signified non-cyclometalation.

**Neutron diffraction study of complex 1:** An exhaustive search<sup>[26]</sup> of the Cambridge Structural Database for neutron structures that contain both C–H and F–C bonds in any capacity afforded eight structures (see the Supporting Information), but none of the associated papers report any C–H...F–C contacts. Therefore the controversial C–H...F–C interaction has been characterized by neutron diffraction for the first time in this study. A perspective view of complex **1**, determined from a neutron diffraction experiment carried out at 20 K to minimize disorder of the *t*Bu and  $\text{CF}_3$  moieties, is shown in Figure 1. As listed in Table 1, there is generally good correlation between the structural parameters derived from the neutron and X-ray<sup>[21]</sup> analyses. The zirconium center resides in a distorted trigonal bipyramidal environment and is chelated by the phenolate-pyridine carbanion [O,N,C] ligand with axial O and C(aryl) and equatorial N and C(benzyl) atoms. Upon initial inspection, the most unusual feature of the structure is the “*anti,anti*” orientation of the benzyl groups (see below). The short  $\text{Zr}\cdots\text{C}_{\text{ipso}}$ (benzyl) separations and acute  $\text{Zr}-\text{C}-\text{C}_{\text{ipso}}$ (benzyl) angles are indicative of  $\eta^2$ -coordination to the metal.

Saliently, the neutron diffraction study of **1** enables the location of hydrogen atoms to be accurately determined. Of special concern is the methylene hydrogen atoms H28B and H35A, which point towards the  $\text{CF}_3$  unit and particularly F1. The observed H...F distances and C–H...F angles (Table 1) are entirely consistent with C–H...F–C interactions as proposed in previously reported X-ray crystal structures.<sup>[14]</sup> Stronger C–H...F–C contacts have been observed in the X-ray crystal structures of 4-fluoroethynylbenzene<sup>[14c]</sup> and an amine adduct of  $\text{B}(\text{C}_6\text{F}_5)_3$ <sup>[14k]</sup> (H...F 2.26 and 2.20 Å; C–H...F 140 and 151°, respectively). For the methylene groups, apparent elongation of the C–H bonds which interact with F1 (1.109(10) and 1.102(7) Å for C28–H28B and C35–H35A, respectively; cf. 1.094(5) Å for both C28–H28A and C35–H35B) is very minor and firm conclusions should not be drawn, while the H–C–H angles (109.5(5) and 110.4(5)°) are normal. This



Scheme 1. [a]  $\text{Zr}(\text{CH}_2\text{Ph})_2$  replaced by  $\text{ZrCl}_2(\text{thf})$  (conditions:  $[\text{Zr}(\text{CH}_2\text{Ph})_2\text{Cl}_2(\text{Et}_2\text{O})_2]$  in toluene/THF).

$R^1$	$R^2$	$R^3$	M
$\text{CF}_3$	$\text{CF}_3$	H	Zr ( <b>1</b> ), Ti ( <b>9</b> )
$\text{CF}_3$	H	F	Zr ( <b>2</b> ), Ti ( <b>10</b> )
Me	H	Me	Zr ( <b>3</b> ), Ti ( <b>11</b> )
H	$\text{CF}_3$	H	Zr ( <b>4</b> )
H	H	H	Zr ( <b>5</b> ), Zr <sup>[a]</sup> ( <b>7</b> )
F	$\text{CF}_3$	H	Zr ( <b>6</b> ), Zr <sup>[a]</sup> ( <b>8</b> ), Ti ( <b>12</b> )

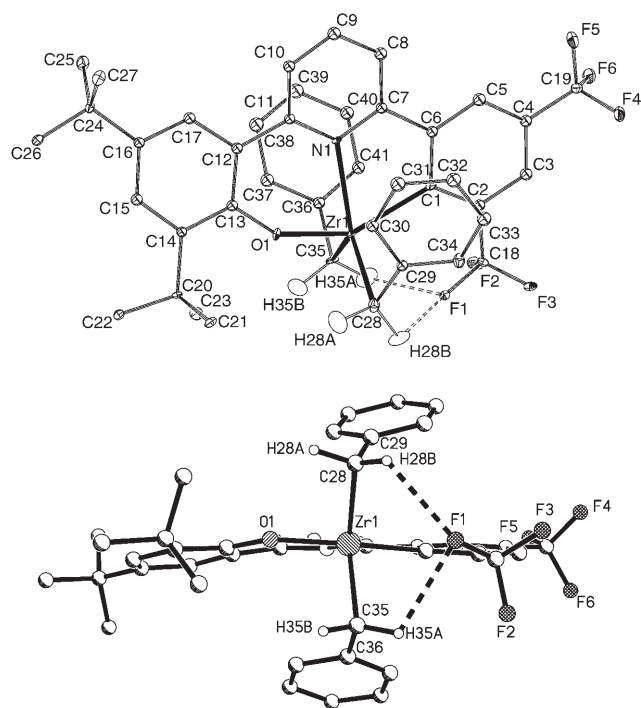


Figure 1. Top: Perspective view of **1** from the neutron diffraction study (50% probability ellipsoids), showing selected hydrogen atoms. Bottom: View along the Zr1–N1 vector.

Table 1. Comparison of selected bond lengths [Å] and angles [°] from neutron and X-ray crystallographic analyses of complex **1**.

	Neutron	X-ray <sup>[a]</sup>
Zr1–C1	2.338(3)	2.330(3)
Zr1–N1	2.426(3)	2.391(2)
Zr1–O1	1.963(3)	1.952(2)
Zr1–C28	2.343(3)	2.276(3)
Zr1...C29	2.722(2)	2.729(3)
Zr1–C35	2.327(3)	2.267(3)
Zr1...C36	2.821(3)	2.765(3)
F1...H28B	2.572(6)	2.471
F1...C28	3.026(4)	2.996(3)
F1...H35A	2.607(5)	2.592
F1...C35	3.132(3)	3.115(3)
C13–O1–Zr1	147.3(2)	147.3(2)
C29–C28–Zr1	87.8(2)	90.7(2)
C36–C35–Zr1	92.0(2)	92.8(2)
F1...H28B–C28	103.3(4)	113.8
F1...H35A–C35	108.2(3)	114.0

[a] The positions of hydrogen atoms were calculated based on a riding model.

lack of obvious geometric distortion, compared with that observed in neutron structures for agostic interactions,<sup>[27]</sup> is perhaps not surprising for very weak hydrogen bonds like C–H...F–C. Along this vein of thought, the importance and applicability of such weak interactions has been debated.<sup>[12]</sup> In the context of this work, since “through-space” coupling within the C–H...F–C moiety has unequivocally been demonstrated by NMR spectroscopy (see below), our objective was to elucidate by neutron diffraction the geometric pa-

rameters associated with the C–H...F–C fragment. This neutron diffraction study may therefore be regarded as a structural reference for intramolecular C–H...F–C interactions that are detectable in solution with potential relevance to polymer–ligand interactions in polyolefin catalysis.

The position of the *ortho*-hydrogen atom H41 relative to F2 is also noteworthy (H41...F2 2.774(7) Å; C41–H41...F2 148.7(4)°). This would be equivalent to the interaction of a  $\gamma$ -hydrogen atom of the polymer chain with the fluorinated ligand and may be compared with a  $\gamma$ -agostic interaction in metallocene catalysts.<sup>[28]</sup> We previously remarked upon the curious inclination of the benzyl groups towards the CF<sub>3</sub> group; namely, the N–Zr–C–C<sub>ipso</sub>(benzyl) dihedral angles are 4.3 and 30.1° (8.4 and 26.5° by X-ray analysis<sup>[21]</sup>). Apart from crystal packing effects, we now propose that it is more appropriate to describe the benzyl ligands as leaning *away* from the adjacent *tert*-butyl unit because the neutron structure has revealed that the methylene hydrogen atoms H28A and H35B are only separated from the H21A and H23C atoms of the *tert*-butyl substituent by 2.148(7) and 2.206(7) Å, respectively. The shortest Zr...F distance of 2.959(4) Å far exceeds the range expected for a significant Zr...F–C interaction.<sup>[29]</sup>

**Comparisons with X-ray crystal structures:** The X-ray crystal structures of several complexes, including those anticipated to display C–H...F–C interactions, have been determined (perspective views of **9**, **10**, and **5** are shown in Figure 2; see the Supporting Information for **4**, **7**, and **12**) and their most informative features are given in Table 2, together with the neutron structural parameters for **1**. All the bis(benzyl) derivatives exhibit trigonal bipyramidal geometry around the metal core, but only complexes **9**, **10**, and **12**, together with **1**, show the two benzyl ligands pointing outwards in a striking “*anti,anti*” configuration; this differs from the normal “*syn,anti*” arrangement observed for **4** and **5** and analogous post-metallocene complexes.<sup>[30]</sup> The  $\eta^2$ -coordination mode of the two benzyl moieties at the titanium center is evident, with the strength of the interaction ranging from strong to rather weak in **9** and **10** (Ti...C<sub>ipso</sub> 2.592(4) to 2.843(2) Å; M–C–C<sub>ipso</sub> 90.0(3) to 102.7(2)°), respectively. Although crystal packing effects cannot be disregarded, we ascribe the recurring yet atypical “*anti,anti*” bis(benzyl) conformation to the highly congested nature of the space at the equatorial plane between the *tert*-butyl and fluorinated substituents such that a metal–( $\eta^2$ -benzyl) interaction cannot be accommodated.

The shortest M...F distances are also listed in Table 2. Significant Zr...F contacts have been reported for a “hemilabile” or “active” ligand,<sup>[4,29]</sup> and Gade and co-workers have structurally characterized zirconium derivatives supported by 2-fluorophenyl-substituted tripodal trisilyl-amido ligands which display noncovalent Zr...F coordination (2.511(2) and 2.535(5) Å).<sup>[31]</sup> Undoubtedly, the M...F separations observed in this work, especially for titanium (>3.15 Å), are excessively long to be considered even as weak interactions. This supports our view that the C–H...F–C coupling detected by NMR spectroscopy is not a consequence of M...F contacts.

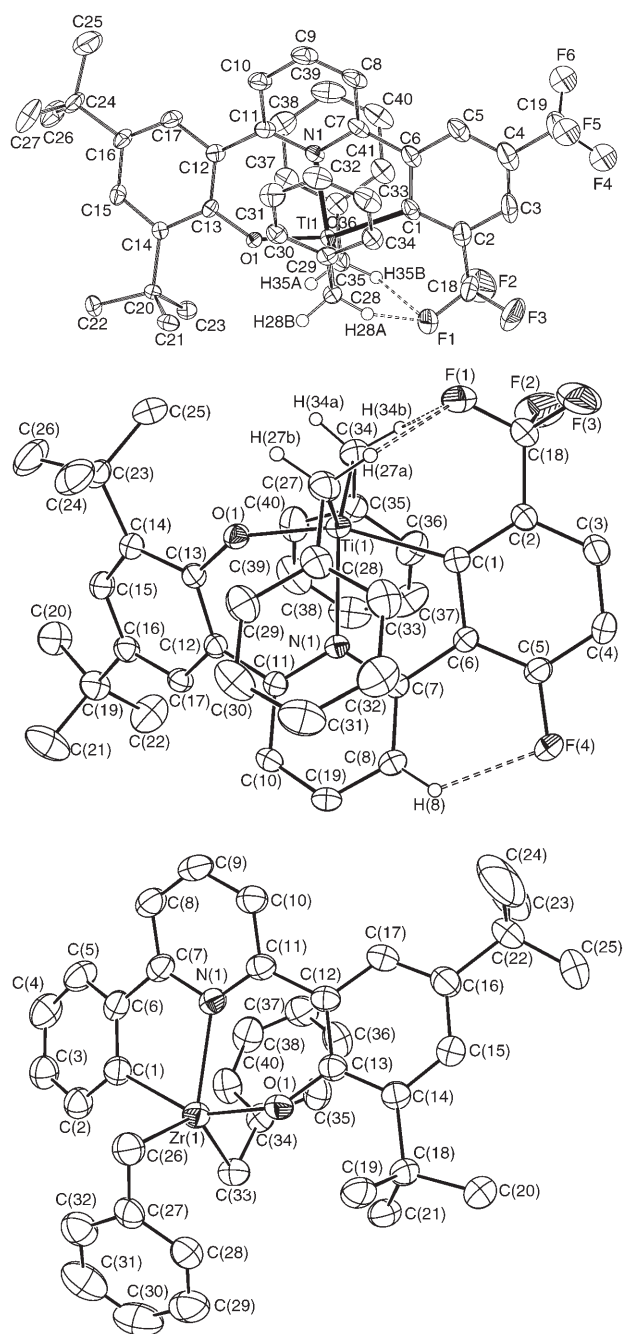


Figure 2. Perspective views of **9** (top, 50% probability ellipsoids), **10**, and **5** (middle and bottom, respectively, 30% probability ellipsoids), showing selected hydrogen atoms as white spheres (positions were calculated based on the riding model).

We wish to emphasize that the following discussion on C–H...F–C interactions is based on calculated hydrogen positions and should be treated cautiously, except when referring to the neutron structural data of **1**. Allowing for this caveat, the H...F (and C...F) distances and C–H...F angles in **9** and **10** between two of the methylene hydrogen atoms and a fluorine atom of the CF<sub>3</sub> group are consistent with the presence of C–H...F–C interactions and in fact these contacts (e.g. H...F 2.39 and 2.43 Å; C–H...F 125 and 123°, re-

spectively) appear to be slightly stronger than in **1**. It is appropriate to remark that a H...F separation of 2.55 Å is apparent in **12** between a methylene hydrogen and the *ortho*-fluorine atom of the aryl carbanion moiety. However, H...F NMR coupling is not observed in solution and we contend that a C...F distance of 3.281(11) Å is excessively long to constitute a significant C–H...F interaction. In contrast to a single fluorine atom, rotation of a CF<sub>3</sub> unit in solution can enable a closer approach and improved alignment between the methylene hydrogen and fluorine atoms to afford stronger and spectroscopically recognizable C–H...F–C interactions. Finally, the existence of a strong intraligand C–H...F contact (H(8)...F(4) 2.19 Å; C(8)–H(8)...F(4) 120°) between a pyridyl hydrogen atom and the distal fluorine atom in the structure of **10**, observable in solution by NMR spectroscopy, is noted.

**Characterization by NMR spectroscopy:** Our preliminary report<sup>[21]</sup> presented direct evidence for the existence in solution of weak intramolecular C–H...F–C interactions in **1** (plus its benzyl cation) and **9**, obtained by using a variety of multinuclear NMR spectroscopic methods, including decoupling, <sup>1</sup>H–<sup>19</sup>F 2D correlation and <sup>1</sup>H/<sup>19</sup>F NOE difference experiments. In this work, detailed spectroscopic characterization of the related complexes **2** and **10** also signify comparable C–H...F–C coupling phenomena between one of the diastereotopic methylene hydrogen atoms and the CF<sub>3</sub> substituent proximal to the metal. For example, complex **2** (Figure 3; see the Supporting Information for **10**) displays an overlapping doublet of quartets at 3.09 ppm (<sup>2</sup>J<sub>H,H</sub> = 9.5, <sup>1</sup>J<sub>H,F</sub> = 3.6 Hz) in the <sup>1</sup>H NMR spectrum for one of the diastereotopic methylene hydrogen atoms, which collapses to a normal doublet upon <sup>19</sup>F decoupling. Furthermore, a quartet at 70.6 ppm (<sup>2</sup>J<sub>C,F</sub> = 6.5 Hz) in the <sup>13</sup>C{<sup>1</sup>H} NMR spectrum for the CH<sub>2</sub> group, plus characteristic sharpening of the downfield <sup>19</sup>F NMR signal at –56.3 ppm only, relative to the <sup>1</sup>H-coupled version, are observed. In addition, strong intraligand H...F coupling (11.3 Hz for **2** and **10**; assignable as <sup>1</sup>J<sub>H,F</sub> rather than <sup>5</sup>J<sub>H,F</sub>) between a pyridyl hydrogen and the distal fluorine atom is apparent.

As expected, C–H...F–C coupling (formally <sup>5</sup>J<sub>H,F</sub>) is undetected for **12** bearing a single fluorine atom at the *ortho*-σ-carbanion position because the H...F separation is excessively long, although the <sup>13</sup>C NMR signal for the methylene carbon atoms at 96.3 ppm exhibits <sup>19</sup>F coupling (formally <sup>4</sup>J<sub>C,F</sub> = 3.3 Hz) by a through-bond mechanism [a through-space process is discounted because the Ti...F separation of 3.469(7) Å is excessively long]. The implication of this is important: if the J<sub>C,F</sub> and J<sub>H,F</sub> couplings in **9** and **10** occur by similar through-bond processes, the corresponding <sup>5</sup>J<sub>C,F</sub> (and <sup>6</sup>J<sub>H,F</sub>) values should be smaller. However, the actual coupling constants are larger, which provides further support for the “through-space” interpretation (i.e. <sup>2</sup>J<sub>C,F</sub> and <sup>1</sup>J<sub>H,F</sub>). Incidentally, through-space coupling between the methylene hydrogen atoms and the *ortho*-methyl group in **3** and **11** is not perceived; while C–F bonds are longer, such interactions would also lack an electrostatic basis. As manifested in the

Table 2. Comparison of selected bond lengths [Å] and angles [°] for molecular structures of bis(benzyl) complexes.<sup>[a]</sup>

	<b>1</b> ( <i>o</i> -CF <sub>3</sub> )	<b>9</b> ( <i>o</i> -CF <sub>3</sub> )	<b>10</b> ( <i>o</i> -CF <sub>3</sub> )	<b>12</b> ( <i>o</i> -F) <sup>[b]</sup>	<b>5</b> ( <i>o</i> -H)
M–C(carbanion)	2.338(3)	2.207(4)	2.210(2)	2.174(9)	2.275(4)
M–CH <sub>2</sub>	2.343(3), 2.327(3)	2.128(4), 2.135(4)	2.118(2), 2.121(2)	2.069(10), 2.093(10)	2.276(4), 2.286(4)
M···C <sub>ipso</sub> (benzyl)	2.722(2), 2.821(3)	2.592(4), 2.765(4)	2.696(2), 2.843(2)	2.669(11), 2.732(11)	2.808(4), 2.587(4)
M–C–C <sub>ipso</sub> (benzyl)	87.8(2), 92.0(2)	90.0(3), 98.5(3)	95.6(2), 102.7(2)	96.3(6), 98.6(6)	94.4(2), 84.4(2)
M···F	2.959(4)	3.231(3)	3.153(4)	3.469(7)	
H···F	2.572(6), 2.607(5)	2.385, 2.595	2.427, 2.494, 2.189 <sup>[d]</sup>	2.551, 2.887	
C···F <sup>[c]</sup>	3.026(4), 3.132(3)	3.064(5), 3.194(5)	3.069(3), 3.072(3), 2.770(3) <sup>[d]</sup>	3.281(11), 3.516(11)	
C–H···F <sup>[c]</sup>	103.3(4), 108.2(3)	125.1, 119.0	123.3, 118.0, 119.7 <sup>[d]</sup>		

[a] Determined by X-ray crystallography (positions of hydrogen atoms were calculated based on the riding model) except **1** (neutron diffraction); the R<sup>1</sup> group *ortho* to the C(carbanion) atom is given in parentheses. [b] Only the titanium atom was refined anisotropically. [c] The parameters are listed in sequence with respect to the above cell. [d] Intraligand C–H···F interaction.

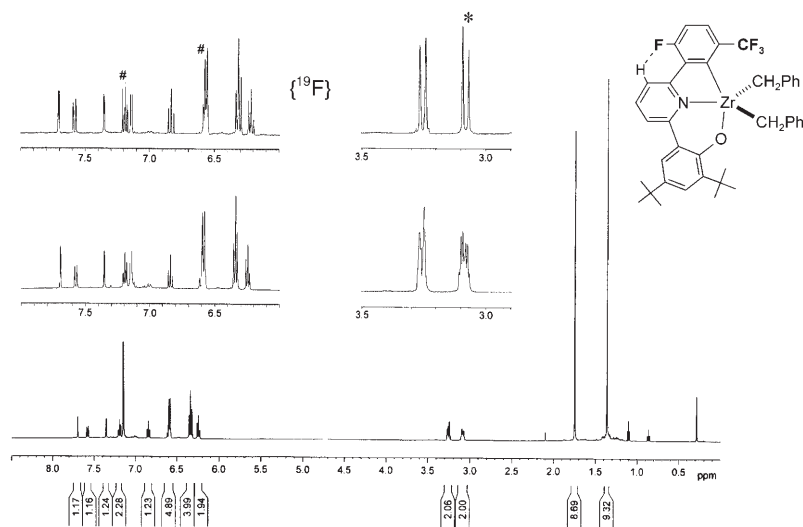


Figure 3. <sup>1</sup>H NMR spectra (400 MHz, C<sub>6</sub>D<sub>6</sub>) of **2**, demonstrating the effects of <sup>19</sup>F decoupling upon the diastereotopic methylene and aromatic hydrogen resonances (\* and # refer to decoupling from CF<sub>3</sub> and F groups, respectively).

molecular structures, the η<sup>2</sup>-coordination modes of the benzyl groups are indicated for all complexes by diminished <sup>2</sup>J<sub>H,H</sub> (< 10 Hz) and large <sup>1</sup>J<sub>C,H</sub> (> 125 Hz) values, plus the high-field shift of the *ortho*-phenyl resonances (e.g. for **9** in C<sub>6</sub>D<sub>6</sub>: 8.3 and 138.9 Hz; 6.44 ppm respectively).<sup>[32]</sup>

**Evaluation of spectroscopic and structural parameters for C–H···F–C interactions:** To acquire a greater insight into the nature of C–H···F–C interactions, we have attempted to

correlate the spectroscopic and structural data and make relevant comparisons with previous investigations (Table 3). While <sup>2</sup>J<sub>C,F</sub> values appear comparable (5.3–6.5 Hz), the <sup>1</sup>J<sub>H,F</sub> values indicate that the C–H···F–C contacts in the titanium derivatives (1.2 and 1.6 Hz) are weaker than those in the zirconium congeners (3.3 and 3.6 Hz). Overall, the anticipated spectroscopy–structure relationship is not apparent, for example, the H···F distances are unpredictably longer for zirconium, although it is apt to consider the relative inaccuracies of the X-ray structural data for the titanium complexes. Notwithstanding this, a very tentative correlation

may exist between **9** and **10**, for which slightly stronger coupling in **9** is accompanied by marginally shorter H···F and C···F separations.

We note two literature reports that have proposed related intramolecular C–H···F coupling in solution in organometallic complexes (Table 3). Van Eldik, Goldberg, and co-workers<sup>[14g]</sup> have studied the spectroscopic and structural properties of [Tp(CF<sub>3</sub>)<sub>2</sub>PtMe<sub>3</sub>] and tentatively suggested the presence of weak through-space C–H···F–C coupling (<sup>1</sup>J<sub>H,F</sub> = 1.8

Table 3. Comparison of selected NMR spectroscopic data<sup>[a]</sup> showing intramolecular C–H···F–C coupling and associated structural parameters.<sup>[b]</sup>

	<sup>1</sup> H: dq [ppm]	<sup>1</sup> J <sub>H,F</sub> [Hz]	<sup>13</sup> C{ <sup>1</sup> H}: q [ppm]	<sup>2</sup> J <sub>C,F</sub> [Hz]	<sup>19</sup> F [ppm]	Mean H···F [Å]	Mean C···F [Å]	Mean C–H···F [°]
<b>1</b>	3.09	3.3	70.5	5.9	–58.1	2.589(6)	3.079(4)	105.8(4)
<b>2</b>	3.09 <sup>[c]</sup>	3.6	70.6 <sup>[d]</sup>	6.5	–56.3			
<b>9</b>	4.00	1.2	96.2	5.3	–56.5	2.49	3.13	122
<b>10</b>	4.04	1.6	95.5	5.9	–55.0	2.46	3.07	121
[Tp(CF <sub>3</sub> ) <sub>2</sub> PtMe <sub>3</sub> ] <sup>[e,f]</sup>	1.58 <sup>[g]</sup>	1.8	–4.9 <sup>[g]</sup>	3.9	–57.0 <sup>[g]</sup>	2.63	3.14	
[(F–N <sub>3</sub> )ZrMe] <sup>[e,h]</sup>	0.65: q	8.4: <sup>3</sup> J <sub>H,F</sub> (via Zr···F)	47.3	17.6: <sup>2</sup> J <sub>C,F</sub> (via Zr···F)	–121.3			

[a] At 400 (<sup>1</sup>H), 126 (<sup>13</sup>C), and 376 (<sup>19</sup>F) MHz in C<sub>6</sub>D<sub>6</sub> unless otherwise stated. [b] From X-ray crystallography (the positions of hydrogen atoms were calculated based on the riding model), except **1** (neutron diffraction). [c] 500 MHz. [d] 151 MHz. [e] At 200 (<sup>1</sup>H), 63 (<sup>13</sup>C), and 188 (<sup>19</sup>F) MHz. [f] See ref. [14g]; Tp(CF<sub>3</sub>)<sub>2</sub> = HB[3,5-bis(trifluoromethyl)pyrazolyl]<sub>3</sub>; in [D<sub>6</sub>]acetone. [g] Septet resonance. [h] See reference [31a]; (F–N<sub>3</sub>) = HC[SiMe<sub>2</sub>N(F–C<sub>6</sub>H<sub>4</sub>)<sub>3</sub>].

and  $^2J_{\text{C,F}} = 3.9$  Hz in  $[\text{D}_6]$ acetone; c.f. **9** and **10**) between the methyl groups and the attendant  $\text{CF}_3$  substituents which point towards them. In contrast, Gade and co-workers have described the tripodal amido-ligated methylzirconium derivative  $[(\text{F-N}_3)\text{ZrMe}]$ ,<sup>[31a]</sup> the larger coupling constants are proposed to occur through  $\text{Zr}\cdots\text{F}$  coordination and are assigned to  $^3J(\text{H-C-Zr}\cdots\text{F})$  and  $^2J(\text{C-Zr}\cdots\text{F})$  (8.4 and 17.6 Hz, respectively), as evidenced by the short  $\text{Zr}\cdots\text{F}$  contact (2.535(5) Å) in the crystal structure of the chloro-bridged analogue.<sup>[31b]</sup> In addition, there is an extended history of investigations into “long-range”/through-space  $\text{C-H}\cdots\text{F-C}$  coupling in fluorinated organic molecules.<sup>[33]</sup>

Density functional theory (DFT) calculations have been successfully utilized by Fujita and co-workers to analyze the structures of FI catalysts and active species.<sup>[8e–g]</sup> We have performed DFT calculations using the Gaussian program to investigate the complexes reported in this work and to make comparisons with the FI catalysts (see the Supporting Information for details).<sup>[34]</sup> First, the structure calculated for **1** was observed to match excellently the neutron and X-ray crystallographic analyses. The calculated distances between the  $\alpha$ -hydrogen atoms of each benzyl group and the nearest fluorine atom of the  $\text{CF}_3$  group are 2.447 and 2.549 Å, which equate to estimated electrostatic energies (ES) of  $-29.4$  and  $-28.7$  kJ mol<sup>-1</sup>, respectively. Second, DFT calculations on the alkyl cationic complex derived from **1** (alkyl = *n*-propyl as a model for the polymer chain), which is widely regarded as the catalytically active species, have been undertaken. Interestingly, the predicted structure exhibits a weak interaction with a distance of 2.606 Å between one of the fluorine atoms and a  $\beta$ -hydrogen atom of the alkyl chain (see the Supporting Information). The ES associated with this interaction is estimated to be  $-31.6$  kJ mol<sup>-1</sup>, which is comparable to the predicted ES of approximately  $-30$  kJ mol<sup>-1</sup> for the corresponding *ortho*-F $\cdots$ H( $\beta$ ) contacts in alkyl cationic FI catalysts.<sup>[8e]</sup>

### Ethylene polymerization and copolymerization studies:

The complexes described in this work have been evaluated as catalysts for the polymerization of ethylene. Importantly, our preliminary investigations in conjunction with methyl alumoxane (MAO) (conditions: 25 °C, 5 min, 1 atm ethylene

feed, 5  $\mu\text{mol}$  catalyst, 1000 equiv MAO, 20 mL toluene) indicated that catalysts bearing fluorinated substituents adjacent to the metal cleft display superior activities (units: g-(polymer)mmol(catalyst)<sup>-1</sup>h<sup>-1</sup>). For zirconium derivatives, the activity of complex **1** (260 gmmol<sup>-1</sup>h<sup>-1</sup>) is incomparably higher than those of **4** and **5** (11 and 4 gmmol<sup>-1</sup>h<sup>-1</sup>, respectively) with non-fluorinated substituents, while for the THF adducts, **8** is noticeably more active than **7** (595 and 150 gmmol<sup>-1</sup>h<sup>-1</sup>, respectively). The large discrepancies in activities cannot solely be rationalized by steric arguments, since complex **3** bearing a methyl substituent in place of a  $\text{CF}_3/\text{F}$  moiety only exhibits moderate activity (70 gmmol<sup>-1</sup>h<sup>-1</sup>). Hence the difference in activities may be attributed to other factors, including the electron-withdrawing effect of multiple  $\text{CF}_3/\text{F}$  groups, which would increase the electrophilicity of the catalytic center. Our initial studies also revealed that for a given ancillary ligand, the titanium catalysts (**9** and **12**: 1060 and 855 gmmol<sup>-1</sup>h<sup>-1</sup>, respectively) are appreciably more active than the zirconium congeners (**1** and **8**: 260 and 595 gmmol<sup>-1</sup>h<sup>-1</sup>, respectively).

Complexes **9** and **12**, together with **1**, were selected as promising candidates for detailed ethylene polymerization and copolymerization studies with propylene and norbornene (Table 4). In addition to MAO, the tests were conducted by using *i*Bu<sub>3</sub>Al/Ph<sub>3</sub>CB(C<sub>6</sub>F<sub>5</sub>)<sub>4</sub> as the co-catalyst. For ethylene polymerization, excellent activities were observed

Table 4. Homo- and copolymerization results.<sup>[a]</sup>

	Reaction	Time [min]	Yield [g]	Activity <sup>[b]</sup>	Co-monomer content [mol %] <sup>[c]</sup>	$T_m$ [°C]
<b>12</b> /MAO	PE	5	1.86	4460		136.5
	EPR	5	1.03	2480	40	
	COC	10	0.98	1180 <sup>[d]</sup>	19.4	no $T_m$ observed
<b>12</b> / <i>i</i> Bu <sub>3</sub> Al/Ph <sub>3</sub> CB(C <sub>6</sub> F <sub>5</sub> ) <sub>4</sub>	PE	5	0.84	2010		134.9
	EPR	5	0.17	410	<10	
	COC	10	0.37	450 <sup>[d]</sup>	20.0	no $T_m$ observed
<b>9</b> /MAO	PE	5	0.74	1770		135.5
	EPR	5	0.46	1120 <sup>[e]</sup>	16.8	
	COC	10	0.81	970 <sup>[e]</sup>		(106.3) <sup>[f]</sup>
<b>9</b> / <i>i</i> Bu <sub>3</sub> Al/Ph <sub>3</sub> CB(C <sub>6</sub> F <sub>5</sub> ) <sub>4</sub>	PE	5	0.58	1400		134.5
	EPR	5	0.31	750 <sup>[e]</sup>	11.1	
	COC	10	0.48	590 <sup>[e]</sup>		(111.0) <sup>[f]</sup>
<b>1</b> /MAO	PE	10	0.32	390		134.7
	EPR	30	0.62	250	5.2	
	COC	10	0.12	140		131.0
<b>1</b> / <i>i</i> Bu <sub>3</sub> Al/Ph <sub>3</sub> CB(C <sub>6</sub> F <sub>5</sub> ) <sub>4</sub>	PE	10	0.69	830		133.3
	EPR	30	1.39	550	17.5	
	COC	10	0.20	240		129.0

[a] Conditions: 25 °C, 1 atm olefin feed, toluene (250 mL), catalyst (5  $\mu\text{mol}$ ), co-cat. MAO (1.25 mmol) or *i*Bu<sub>3</sub>Al (0.25 mmol)/Ph<sub>3</sub>CB(C<sub>6</sub>F<sub>5</sub>)<sub>4</sub> (1.2 equiv vs. cat.), PE (ethylene polymerization): C<sub>2</sub> = 100 L h<sup>-1</sup>, EPR (ethylene/propylene copolymerization): C<sub>2</sub>/C<sub>3</sub> = 100/100 L h<sup>-1</sup>, COC (ethylene/norbornene copolymerization): C<sub>2</sub> = 50 L h<sup>-1</sup>; NB = 1 g. [b] g(polymer)mmol(catalyst)<sup>-1</sup>h<sup>-1</sup>. [c] C<sub>3</sub> and NB contents were determined by <sup>1</sup>H (except for **12**: IR) and <sup>13</sup>C NMR analysis, respectively. [d]  $M_w$  and  $M_w/M_n$  values with MAO ( $1.51 \times 10^7$  and 2.66, respectively) and borate ( $2.00 \times 10^7$  and 1.52, respectively) co-catalysts were determined by GPC. [e]  $M_v$  values were determined from the intrinsic viscosity  $[\eta]$  of the polymer in decalin at 135 °C and calculated using  $[\eta] = 6.2 \times 10^{-4} M_v^{0.7}$  to be (1.34, 2.33, 1.73, and 1.37)  $\times 10^6$ , respectively, upon descending the column; all other polymers were insoluble under the analysis conditions, presumably as a result of their very high molecular weights. [f] Very small peaks.

with the titanium catalysts, up to  $4460 \text{ g mmol}^{-1} \text{ h}^{-1}$  for **12**/MAO (considering the Al/Ti ratio is only 250). Like many of the experiments, the resultant polymer is insoluble under the conditions used for intrinsic viscosity analysis ( $135^\circ\text{C}$  in decalin), presumably due to its very high molecular weight ( $M_v > 3 \times 10^6$ ).

Interesting results were obtained for these catalysts in ethylene/propylene copolymerization reactions. The **12**/MAO system displays impressive activities that are superior to **9**/MAO and the molecular weight of the poly(ethylene-co-propylene) (EPR) produced is also higher such that the polymer is insoluble and unsuitable for  $^1\text{H}$  NMR determination of propylene (C3) content. Hence IR analysis was employed to show that 40 mol % of propylene is incorporated into the EPR prepared using **12**/MAO, compared with 17 mol % (from  $^1\text{H}$  NMR) incorporated using **9**/MAO. The ability of the **12**/MAO system, with a single fluorine atom adjacent to the metal rather than a  $\text{CF}_3$  substituent, to incorporate high C3 content into the copolymer (FI catalysts can incorporate up to about 20 mol %<sup>[8e,g,35]</sup>) is striking and may be ascribed to the increased availability of space around the active site which facilitates the coordination/insertion of sterically demanding monomers.

The **12**/*i*Bu<sub>3</sub>Al/Ph<sub>3</sub>CB(C<sub>6</sub>F<sub>5</sub>)<sub>4</sub> system yielded lower activities and decreased C3 content for EPR, the latter indicated by IR analysis (<10 mol %) and the appearance of  $T_m$  ( $114.6^\circ\text{C}$ ) for the resultant polymer. In general, the use of the *i*Bu<sub>3</sub>Al/Ph<sub>3</sub>CB(C<sub>6</sub>F<sub>5</sub>)<sub>4</sub> co-catalyst resulted in inferior activities and suppressed co-monomer incorporation. Fujita and co-workers have investigated the contrasting effects of the MAO and *i*Bu<sub>3</sub>Al/Ph<sub>3</sub>CB(C<sub>6</sub>F<sub>5</sub>)<sub>4</sub> co-catalysts upon the performance of FI catalysts,<sup>[8i,35]</sup> and concluded that the imine moiety is readily reduced by *i*Bu<sub>3</sub>Al to the amine and that the reduced catalytic species is typically less active than the MAO-activated analogue but tends to produce extremely high molecular weight polymers. In this work, while the pyridine group should be more resistant to electrophilic attack by *i*Bu<sub>3</sub>Al, we note that reduction of the titanium center is possible (see below) and there is a precedence for such transformations in related ligand systems.<sup>[36]</sup> Intriguingly, this trend is reversed for the zirconium catalyst; the **1**/*i*Bu<sub>3</sub>Al/Ph<sub>3</sub>CB(C<sub>6</sub>F<sub>5</sub>)<sub>4</sub> system displays improved activities as well as greater C3 incorporation (17.5 versus 5.2 mol %) compared with **1**/MAO. The zirconium active sites are evidently less susceptible to reduction processes, although reasons for the superior performance are unclear.

The abilities of these catalysts to mediate ethylene/norbornene (C2/NB) copolymerizations are also noteworthy. The activity of **12**/MAO ( $1180 \text{ g mmol}^{-1} \text{ h}^{-1}$ ) remains very respectable and is greater than that for **9**/MAO with higher molecular weights. Significantly, both **12** and **9** with MAO or *i*Bu<sub>3</sub>Al/Ph<sub>3</sub>CB(C<sub>6</sub>F<sub>5</sub>)<sub>4</sub> can produce very high molecular weight C2/NB copolymers (COC: cyclic olefin copolymers), as shown by lower  $T_m$  values relative to those of the PE samples. Furthermore, **12**/MAO and **12**/*i*Bu<sub>3</sub>Al/Ph<sub>3</sub>CB(C<sub>6</sub>F<sub>5</sub>)<sub>4</sub> afford C2/NB elastomers with no  $T_m$  value and excellent NB content (19.4 and 20.0 mol % NB, respectively). The elevated

degree of NB incorporation for **12**, with a sterically accessible (relative to **9**) and highly electrophilic catalytic center, surpasses the performance of the metallocene *rac*-[Et-(Ind)<sub>2</sub>ZrCl<sub>2</sub>] (Ind=indenyl) and begins to approach that of the bis(pyrrrole-imine) titanium catalyst system developed by Fujita and co-workers (8.3 and 26.5 mol % NB, respectively under similar conditions<sup>[37]</sup>). In contrast, the zirconium catalyst **1** exhibits poor NB incorporation, as implied by the high PE-like  $T_m$  values.

The narrow molecular weight distributions (low  $M_w/M_n$  values) for **12**/MAO and **12**/*i*Bu<sub>3</sub>Al/Ph<sub>3</sub>CB(C<sub>6</sub>F<sub>5</sub>)<sub>4</sub> (2.66 and 1.52, respectively) are entirely consistent with active-site uniformity. In contrast, under small-scale polymerization conditions accompanied by the appearance of an exotherm, **9** produces PE samples with broad molecular weight distributions ( $M_w/M_n > 10$ ). We note that a ligand-transfer degradation pathway involving the FI catalyst [L<sub>2</sub>TiMe]<sup>+</sup> (L = *N*-(3-*tert*-butylsalicylidene)pentamethylammonium) and AlMe<sub>3</sub>, resulting in the formation of LAlMe<sub>2</sub> and an unidentified titanium species that is less active, has been elucidated.<sup>[38]</sup> We suggest that in this system, similar transmetalation reactions between the Al-C(alkyl) and Ti-C(aryl  $\sigma$ -carbanion) bonds of the co-catalyst and catalytic center, respectively, may transpire at elevated temperatures. The development of these catalysts may therefore be hampered by the fragile nature of the [O,N,C] chelation and particularly the Ti-C(aryl) linkage.

The catalytic capabilities of Group 4 alkyl complexes supported by fluorine- and chlorine-functionalized multi-amido/donor ligands, recently developed by Schrock and co-workers, are of relevance to the issues in this work and warrant discussion. The impressive ability of the diamidoamine-bound cation [(2,6-Cl<sub>2</sub>C<sub>6</sub>H<sub>3</sub>NCH<sub>2</sub>CH<sub>2</sub>)<sub>2</sub>NMe]ZrMe<sup>+</sup> to mediate the living polymerization of 1-hexene has been reported<sup>[39]</sup> and it is interesting to note that the possibility of stabilizing catalytic centers 'via "light" (or transiently dative) coordination of the chloride to the metal' was proposed. In a related system, the impact of *ortho*-fluorine and -chlorine substituents in alkylhafnium cations containing the diamidopyridine ligands [(2,6-X<sub>2</sub>C<sub>6</sub>H<sub>3</sub>NCH<sub>2</sub>)<sub>2</sub>C(2-py)Me]<sup>2-</sup> ([ArX<sub>2</sub>Npy]<sup>2-</sup>; X = F, Cl) upon their 1-hexene polymerization performance has been examined.<sup>[40]</sup> Compared with mesityl, the introduction of the 2,6-Cl<sub>2</sub>- and especially 2,6-F<sub>2</sub>C<sub>6</sub>H<sub>3</sub> group resulted in detrimental activities and accelerated the rate of  $\beta$ -hydride elimination. These observations are seemingly contradictory to the beneficial effects of weak C-H...F-C ligand-polymer interactions espoused by Fujita and co-workers<sup>[8b]</sup> and the present work. However, it is reasonable to point out that there are clear chemical and structural distinctions between the catalytic systems mentioned. Apart from ligand characteristics/geometry and metal environments, the salient difference is the propensity for the *ortho*-fluorine (or chlorine) atoms of the [ArX<sub>2</sub>Npy]<sup>2-</sup> ligands to coordinate to the hafnium center, as illustrated in the respective crystal structures<sup>[40]</sup> (Hf...F 2.443(3) and 2.674(3) Å; Hf...Cl 2.760(3) Å); the fluorine groups in the catalysts reported here and by Fujita and co-workers do not



interact with the titanium/zirconium core. It is well-established that such Hf...F/Cl contacts can increase the steric demand at the active site leading to the suppression of catalytic activity.<sup>[3]</sup> In general, we anticipate that catalytically applicable C–H...F–C polymer–ligand interactions may be pre-empted if the C–F unit(s) can approach the metal (due to a flexible ligand framework) and stronger M...F metal–ligand coordination could occur.

## Conclusion

A family of Group 4 post-metallocene catalysts, supported by fluorine-functionalized tridentate ligands that impose the fluorine group in proximity to the active site, has been designed and synthesized. By employing multinuclear NMR spectroscopy in tandem with neutron and X-ray crystallography, attempts have been made to: 1) elucidate the nature of the intramolecular C–H...F–C interactions in these complexes in solution and in the solid state, and 2) gather evidence to explicitly show that the C–H...F–C coupling occurs “through-space” rather than “through-bond” or by M...F coordination. The performances of the titanium catalysts appended with fluorine substituents are intriguing, with excellent activities, high co-monomer incorporation and considerable effects due to the choice of co-catalyst.

Importantly, a neutron diffraction study of complex **1** has been completed and this constitutes the first time that the structural parameters of weak C–H...F–C interactions have been accurately determined. The observed H...F distances (2.572(6) and 2.607(5) Å) and C–H...F angles (103.3(4) and 108.2(3)°) indicate a moderate-to-weak interaction when compared with previous X-ray crystallographic reports. Indeed, the former are fractionally longer than the sum of the van der Waals radii (2.54 Å) as defined by Rowland and Taylor,<sup>[13]</sup> which is routinely described as a cut-off distance for nonbonded interatomic contacts.<sup>[41]</sup> However weak they may be perceived, we regard the C–H...F–C interactions in this work to be genuine (because the C–H...F–C coupling in solution is tangible) and of relevance with respect to potential applications in olefin polymerization reactions. Namely, these results corroborate Fujita’s proposed *ortho*-F...H( $\beta$ ) contacts and demonstrate that such interactions are experimentally feasible. In essence, we have an authenticated example of a neutron structure containing weak intramolecular C–H...F–C interactions, the geometric parameters of which are (or approach the outer limit of being) translated into NMR-discernible C–H...F–C coupling in solution and which may be consequential for the new concept and development of weak attractive polymer–ligand interactions in polyolefin catalysis.

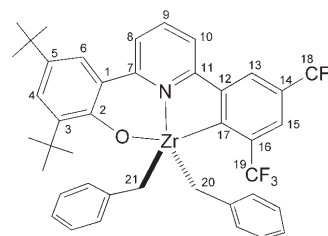
## Experimental Section

**General considerations:** All reactions were performed under nitrogen using standard Schlenk techniques or in a Braun dry-box. All solvents

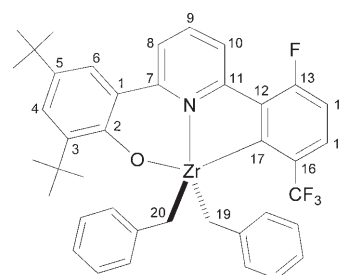
were appropriately dried, distilled, and then degassed prior to use. <sup>1</sup>H and <sup>13</sup>C NMR spectra were recorded at 300 K on a Bruker Avance 600, 500 DRX, 400, or 300 FT-NMR spectrometer (referenced to residual solvent protons). Peak assignments were based on combinations of DEPT-135, 2-D <sup>1</sup>H–<sup>1</sup>H and <sup>13</sup>C–<sup>1</sup>H correlations, and NOE NMR experiments. <sup>19</sup>F NMR spectra were recorded at 300 K on a Bruker Avance 400 spectrometer (with trifluoroacetic acid as external reference). Elemental analyses were performed by Medac Ltd., UK.

The complexes [M(CH<sub>2</sub>Ph)<sub>4</sub>] (M = Ti, Zr)<sup>[42]</sup> and [Zr(CH<sub>2</sub>Ph)<sub>2</sub>Cl<sub>2</sub>(OEt<sub>2</sub>)<sub>n</sub>]<sup>[43]</sup> were prepared according to published procedures. The 2-(2'-methoxyaryl)-6-arylpyridines were prepared by modification of a literature method<sup>[44]</sup> and subsequent demethylation using molten pyridinium chloride<sup>[45]</sup> gave the 2-(2'-hydroxyphenyl)-6-arylpyridine substrates (see the Supporting Information for details).

**General synthetic procedure for the preparation of bis(benzyl) complexes:** 2-(2'-Hydroxyphenyl)-6-arylpyridine substrate in pentane/diethyl ether (5:1) was slowly added to a stirred solution of [M(CH<sub>2</sub>Ph)<sub>4</sub>] in pentane/diethyl ether (5:1) at –78 °C. The reaction mixture was allowed to warm to 25 °C and stirred for 12 h. The resultant solution was filtered, concentrated to about 10 mL, and stored at –15 °C to afford a crystalline solid. Analytically pure products were obtained by recrystallization from pentane (detailed procedures and characterization data for all complexes are provided in the Supporting Information).

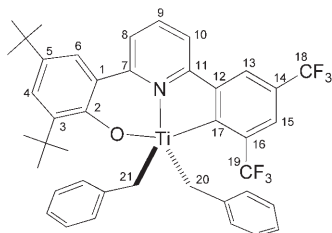


**1:** Orange-red crystals; yield 62%. Elemental analysis calcd (%) for C<sub>41</sub>H<sub>39</sub>F<sub>6</sub>NOZr (766.98): C 64.21, H 5.13, N 1.83; found: C 63.99, H 5.57, N 1.89. <sup>1</sup>H NMR (400 MHz, C<sub>6</sub>D<sub>6</sub>):  $\delta$  = 1.36 (s, 9H; 5-*t*Bu), 1.72 (s, 9H; 3-*t*Bu), 3.09 (dq, *J* = 9.6, <sup>1</sup>*J*<sub>H,F</sub> = 3.3 Hz, 2H; 20'-H and 21'-H), 3.26 (d, *J* = 9.4 Hz, 2H; 20-H and 21-H), 6.18 (t, *J* = 7.3 Hz, 2H; *p*-Ph), 6.25 (t, *J* = 7.7 Hz, 4H; *m*-Ph), 6.54 (d, *J* = 7.4 Hz, 4H; *o*-Ph), 6.57 (d, *J* = 7.9 Hz, 1H; 10-H), 6.77 (t, *J* = 8.0 Hz, 1H; 9-H), 7.25 (d, *J* = 8.0 Hz, 1H; 8-H), 7.40 (d, *J* = 2.3 Hz, 1H; 6-H), 7.60 (s, 1H; 13-H), 7.69 (d, *J* = 2.4 Hz, 1H; 4-H), 7.81 ppm (s, 1H; 15-H); <sup>13</sup>C NMR (126 MHz, C<sub>6</sub>D<sub>6</sub>):  $\delta$  = 31.3 (3-*CMe*<sub>3</sub>), 32.1 (5-*CMe*<sub>3</sub>), 35.0 and 36.1 (*CMe*<sub>3</sub>), 70.5 (q, <sup>2</sup>*J*<sub>C,F</sub> = 5.9 Hz (*J*<sub>C,H</sub> = 133.3 Hz), C-20 and C-21), 118.1 (C-10), 127.6 (C-4), 122.1 (br, C-15), 123.2 (br, C-13), 123.8 (*p*-Ph), 124.4 (C-8), 125.4 (C-6), 129.1 (*o*-Ph), 129.9 (*m*-Ph), 130.8 and 138.5 (q, *J*<sub>C,F</sub> = 31.1 Hz, C-18 and C-19), 136.9 (*i*-Ph), 139.3 (C-9), 189.9 ppm (C-17); <sup>4</sup> carbons: 126.7, 138.1, 142.8, 145.1, 155.3, 159.3, 161.6 ppm; <sup>19</sup>F NMR (376 MHz, C<sub>6</sub>D<sub>6</sub>):  $\delta$  = –58.1 (19-F), –62.6 ppm (18-F).

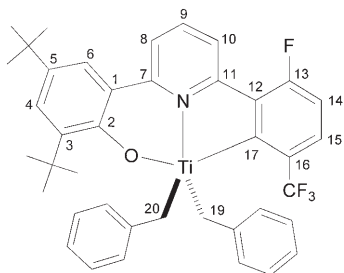


**2:** Orange crystalline solid; yield 75%. Elemental analysis calcd (%) for C<sub>40</sub>H<sub>39</sub>F<sub>4</sub>NOZr (716.97): C 67.01, H 5.48, N 1.95; found: C 66.93, H 5.57, N 2.18. <sup>1</sup>H NMR (400 MHz, C<sub>6</sub>D<sub>6</sub>):  $\delta$  = 1.36 (s, 9H; 5-*t*Bu), 1.75 (s, 9H; 3-

*t*Bu), 3.09 (dq,  $J=9.5$ ,  $^1J_{\text{HF}}=3.6$  Hz, 2H; 19'-H and 20'-H), 3.26 (d,  $J=9.5$  Hz, 2H; 19-H and 20-H), 6.25 (t,  $J=7.3$  Hz, 2H; *p*-Ph), 6.35 (t,  $J=7.4$  Hz, 4H; *m*-Ph), 6.58–6.62 (m, 5H; *o*-Ph and 14-H), 6.85 (t,  $J=8.0$  Hz, 1H; 9-H), 7.19–7.21 (m, 2H; 10-H and 15-H), 7.36 (d,  $J=2.4$  Hz, 1H; 6-H), 7.58 (d,  $J=8.1$  Hz, 1H; 8-H), 7.70 ppm (d,  $J=2.4$  Hz, 1H; 4-H);  $^{13}\text{C}$  NMR (151 MHz,  $\text{C}_6\text{D}_6$ ):  $\delta=31.4$  (3- $\text{CMe}_3$ ), 32.2 (5- $\text{CMe}_3$ ), 35.0 and 36.1 ( $\text{CMe}_3$ ), 70.6 (q,  $^2J_{\text{CF}}=6.5$  Hz, C-19 and C-20), 116.9 (d,  $^2J_{\text{CF}}=27.6$  Hz, C-14), 122.5 (d,  $^2J_{\text{CF}}=22.6$  Hz, C-10), 123.6 (*p*-Ph), 124.3 (C-8), 125.6 (C-6), 127.4 (C-4), 127.9 (C-15, obscured by residual solvent peak), 128.9 (*m*-Ph), 129.9 (*o*-Ph), 132.7 (q,  $J_{\text{CF}}=33.0$  Hz,  $\text{CF}_3$ ), 137.4 (*i*-Ph), 139.2 (C-9), 159.9 (d,  $^2J_{\text{CF}}=7.3$  Hz, C-12), 162.4 (d,  $^1J_{\text{CF}}=265.0$  Hz, C-13), 190.5 ppm (m, C-17);  $^4\sigma$  carbons:  $\delta=127.1$ , 137.8, 142.6, 155.3, 159.8 ppm;  $^{19}\text{F}$  NMR (376 MHz,  $\text{C}_6\text{D}_6$ ):  $\delta=-55.0$  ( $\text{CF}_3$ ),  $-108.6$  (d,  $^1J_{\text{FH}}=11.3$  Hz, 13-F).

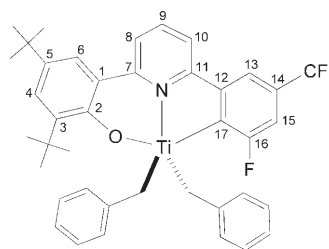


**9:** Dark red crystals; yield 57%. Elemental analysis calcd (%) for  $\text{C}_{41}\text{H}_{39}\text{F}_6\text{NO}_2\text{Ti}$  (723.66): C 68.05, H 5.43, N 1.93; found: C 68.08, H 5.58, N 2.09.  $^1\text{H}$  NMR (400 MHz,  $\text{C}_6\text{D}_6$ ):  $\delta=1.34$  (s, 9H; 5-*t*Bu), 1.77 (s, 9H; 3-*t*Bu), 4.00 (brdq,  $J=8.4$ ,  $^1J_{\text{HF}}=1.2$  Hz, 2H; 20'-H and 21'-H), 4.04 (d,  $J=8.3$  Hz, 2H; 20-H and 21-H), 6.25 (t,  $J=7.2$  Hz, 2H; *p*-Ph), 6.32 (t,  $J=7.1$  Hz, 4H; *m*-Ph), 6.42 (d,  $J=8.3$  Hz, 1H; 10-H), 6.44 (d,  $J=7.3$  Hz, 4H; *o*-Ph), 6.66 (t,  $J=8.0$  Hz, 1H; 9-H), 7.21 (d,  $J=8.0$  Hz, 1H; 8-H), 7.40 (d,  $J=2.1$  Hz, 1H; 6-H), 7.60 (s, 1H; 13-H), 7.70 (d,  $J=2.3$  Hz, 1H; 4-H), 8.12 ppm (s, 1H; 15-H);  $^{13}\text{C}$  NMR (126 MHz,  $\text{C}_6\text{D}_6$ ):  $\delta=31.1$  (3- $\text{CMe}_3$ ), 31.7 (5- $\text{CMe}_3$ ), 34.7 and 35.7 ( $\text{CMe}_3$ ), 96.2 (q,  $^2J_{\text{CF}}=5.3$  Hz ( $J_{\text{CH}}=138.9$  Hz), C-20 and C-21), 116.6 (C-10), 122.8 (br, C-13), 123.2 (br, C-15), 123.4 (C-8), 124.1 (*p*-Ph), 124.4 (C-6), 127.5 (C-4), 127.6 (*m*-Ph), 131.1 and 137.2 (q,  $J_{\text{CF}}=32.5$  and 30.2 Hz resp., C-18 and C-19), 130.5 (*o*-Ph), 137.6 (*i*-Ph), 139.3 (C-9), 193.4 ppm (C-17);  $^4\sigma$  carbons: 127.3, 137.0, 143.1, 144.9, 156.8, 156.9, 161.4 ppm;  $^{19}\text{F}$  NMR (376 MHz,  $\text{C}_6\text{D}_6$ ):  $\delta=-56.5$  (19-F),  $-62.6$  ppm (18-F).



**10:** Dark red crystalline solid; yield 74%. Elemental analysis calcd (%) for  $\text{C}_{40}\text{H}_{39}\text{F}_4\text{NO}_2\text{Ti}$  (673.64): C 71.32, H 5.84, N 2.08; found: C 71.05, H 5.91, N 2.23;  $^1\text{H}$  NMR (400 MHz,  $\text{C}_6\text{D}_6$ ):  $\delta=1.35$  (s, 9H; 5-*t*Bu), 1.79 (s, 9H; 3-*t*Bu), 4.02 (d,  $J=8.4$  Hz, 2H; 19'-H and 20'-H), 4.04 (dq,  $J=8.5$ ,  $^1J_{\text{HF}}=1.6$  Hz, 2H; 19'-H and 20'-H), 6.29 (t,  $J=7.5$  Hz, 2H; *p*-Ph), 6.38 (t,  $J=7.5$  Hz, 4H; *m*-Ph), 6.49 (d,  $J=7.2$  Hz, 4H; *o*-Ph), 6.66–6.74 (m, 2H; 14-H and 9-H), 7.16 (1H; 8-H, fused with residual solvent peak), 7.33 (d,  $J=2.2$  Hz, 1H; 6-H), 7.46–7.51 (m, 2H; 10-H and 15-H), 7.68 ppm (d,  $J=2.3$  Hz, 1H; 4-H);  $^{13}\text{C}$  NMR (126 MHz,  $\text{C}_6\text{D}_6$ ):  $\delta=30.9$  (3- $\text{CMe}_3$ ), 31.5 (5- $\text{CMe}_3$ ), 34.4 and 35.4 ( $\text{CMe}_3$ ), 95.5 (q,  $^2J_{\text{CF}}=5.9$  Hz, C-19 and C-20), 116.3 (d,  $^2J_{\text{CF}}=27.2$  Hz, C-14), 120.8 (d,  $^2J_{\text{CF}}=24.1$  Hz, C-10), 123.0 (C-8), 123.7 (*p*-Ph), 124.4 (C-6), 127.0 (C-4), 127.3 (*m*-Ph),

128.9 (m, C-15), 130.2 (*o*-Ph), 131.4 (q,  $J_{\text{CF}}=30.0$  Hz,  $\text{CF}_3$ ), 136.4 (*i*-Ph), 139.2 (C-9), 159.6 (d,  $^2J_{\text{CF}}=7.6$  Hz, C-12), 161.5 (d,  $^1J_{\text{CF}}=265.4$  Hz, C-13), 193.7 ppm (m, C-17);  $^4\sigma$  carbons:  $\delta=137.9$ , 142.7, 156.6, 156.9 ppm;  $^{19}\text{F}$  NMR (376 MHz,  $\text{C}_6\text{D}_6$ ):  $\delta=-55.0$  ( $\text{CF}_3$ ),  $-108.6$  (d,  $^1J_{\text{FH}}=11.3$  Hz, 13-F).



**12:** Dark red crystals; yield 78%. Elemental analysis calcd (%) for  $\text{C}_{40}\text{H}_{39}\text{F}_4\text{NO}_2\text{Ti}$  (673.64): C 71.32, H 5.84, N 2.08; found: C 71.40, H 6.01, N 2.12.  $^1\text{H}$  NMR (600 MHz,  $\text{C}_6\text{D}_6$ ):  $\delta=1.34$  (s, 9H; 5-*t*Bu), 1.80 (s, 9H; 3-*t*Bu), 4.13 (d,  $J=8.5$  Hz, 2H;  $\text{CH}_2$ ), 4.39 (d,  $J=8.5$  Hz, 2H;  $\text{CH}_2$ ), 6.31 (t,  $J=7.3$  Hz, 2H; *p*-Ph), 6.42–6.44 (m, 5H; *m*-Ph and 10-H), 6.64 (t,  $J=7.9$  Hz, 1H; 9-H), 6.66 (d,  $J=7.3$  Hz, 4H; *o*-Ph), 7.12 (d,  $J=8.0$  Hz, 1H; 8-H), 7.33 (s, 1H; 13-H), 7.35 (d,  $^3J_{\text{HF}}=4.7$  Hz, 1H; 15-H), 7.39 (d,  $J=2.3$  Hz, 1H; 6-H), 7.71 ppm (d,  $J=2.3$  Hz, 1H; 4-H);  $^{13}\text{C}$  NMR (150.9 MHz,  $\text{C}_6\text{D}_6$ ):  $\delta=30.7$  (3- $\text{CMe}_3$ ), 31.5 (5- $\text{CMe}_3$ ), 34.4 and 35.5 ( $\text{CMe}_3$ ), 96.3 (d,  $^4J_{\text{CF}}=3.3$  Hz,  $\text{CH}_2$ ), 112.6 (dq,  $^2J_{\text{CF}}=36.2$ ,  $^3J_{\text{CF}}=3.6$  Hz, C-15), 115.4 (m, C-13), 116.0 (C-10), 122.8 (C-8), 123.9 (*p*-Ph), 124.2 (C-6), 127.0 (C-4), 127.8 (*m*-Ph, obscured by residual solvent peak), 131.0 (*o*-Ph), 131.9 (q,  $^1J_{\text{CF}}=32.5$  Hz,  $\text{CF}_3$ ), 135.8 (*i*-Ph), 139.1 (C-9), 145.4 (d,  $^3J_{\text{CF}}=20.8$  Hz, C-12), 166.1 (d,  $^1J_{\text{CF}}=233.9$  Hz, C-16), 181.1 ppm (d,  $^2J_{\text{CF}}=59.4$  Hz, C-17);  $^4\sigma$  carbons: 127.1, 136.8, 142.7, 156.6, 156.9, 161.5 ppm;  $^{19}\text{F}$  NMR (376 MHz,  $\text{C}_6\text{D}_6$ ):  $\delta=-62.1$  ( $\text{CF}_3$ ),  $-98.5$  ppm (16-F).

**Neutron diffraction study:** A  $1.5 \times 1.3 \times 1.0$  mm $^3$  single crystal, suspended between two quartz wool plugs in a glass capillary flushed with nitrogen, was mounted on the Very-Intense Vertical-Axis Laue Diffractometer (VIVALDI) at the Institut Laue-Langevin (ILL), Grenoble, France in a helium-flow cryostat and cooled to  $T=20.0(5)$  K (Table 5). Laue diffraction patterns were obtained using a polychromatic thermal-neutron beam with a large solid-angle (8 sterad) cylindrical image-plate detector<sup>[46]</sup> to increase the detected diffracted intensity by one-to-two orders of magnitude compared with a conventional monochromatic experiment. Fifteen Laue diffraction patterns, successive patterns separated by  $5\text{--}20^\circ$  in  $\phi$  rotation of the crystal perpendicular to the incident neutron beam, were collected over a  $170^\circ$  range at  $T=20.0(5)$  K, each pattern requiring a 6 hour acquisition time with blue Fuji image plates.

The images were indexed by using the LAUEGEN program of the Daresbury Laboratory Laue Suite<sup>[47]</sup> and the reflections were integrated using the local INTEGRATE+ program which uses a two-dimensional version of the minimum  $\sigma(I)/I$  algorithm.<sup>[48]</sup> The individual reflections were corrected for absorption using the calculated (wavelength-dependent) absorption coefficient,  $0.08437\lambda + 0.08936$  mm $^{-1}$  (transmission range: 0.717–0.869). The reflections were normalized to a common wavelength using a curve derived by comparing equivalent reflections and multiple observations with the LAUENORM program.<sup>[49]</sup> Only reflections in the wavelength range of 0.9–2.2 Å were retained to yield a total of 23 578 single and 6641 unique reflections. Fourier difference analysis allowed unambiguous identification and location of the hydrogen atoms. The model was refined by full-matrix least-squares refinement using SHELXL-97.<sup>[50]</sup> Positional and anisotropic displacement parameters were refined for all atoms except the phenyl carbon atoms for which only the positional and isotropic displacement parameters were refined. This atom-selective difference in the treatment of displacement parameters was applied in order to optimize the refinement data/parameter ratio to obtain the most accurate parameters for the most scientifically important

Table 5. Crystal data and structure refinement for **1**.

empirical form.	C <sub>41</sub> H <sub>39</sub> F <sub>6</sub> NOZr
form. wt.	766.98
<i>T</i> [K]	20.0(5)
accepted wavelength [Å]	0.9–2.2
crystal system	triclinic
space group	<i>P</i> 1
unit cell dimensions	
<i>a</i> [Å]	9.613(2)
<i>b</i> [Å]	11.860(2)
<i>c</i> [Å]	16.928(3)
$\alpha$ [°]	109.37(3)
$\beta$ [°]	90.88(3)
$\gamma$ [°]	97.88(3)
<i>V</i> [Å <sup>3</sup> ]	1799.7(6)
<i>Z</i>	2
$\rho_{\text{calcd}}$ [g cm <sup>-3</sup> ]	1.412
absorption coefficient [mm <sup>-1</sup> ]	0.08437 $\lambda$ + 0.08936
<i>F</i> (000)	366
crystal size [mm <sup>3</sup> ]	1.50 × 1.30 × 1.00
$\theta$ range for data collection [°]	3.77–45.81
index range	−11 ≤ <i>h</i> ≤ 11, −18 ≤ <i>k</i> ≤ 18, −26 ≤ <i>l</i> ≤ 20
reflections collected	23493
independent reflections	6641 [ <i>R</i> <sub>int</sub> = 0.1899]
completeness to $\theta = 45.81^\circ$ [%]	43.5
absorption correction	Gaussian integration
max. and min. transmission	0.869 and 0.717
refinement method	full-matrix least-squares on <i>F</i> <sup>2</sup>
data/restraints/parameters	6641/0/667
GOF on <i>F</i> <sup>2</sup>	1.117
final <i>R</i> indices [ <i>I</i> > 2 $\sigma$ ( <i>I</i> )]	<i>R</i> <sub>1</sub> = 0.0642, <i>wR</i> <sub>2</sub> = 0.1037
<i>R</i> indices (all data)	<i>R</i> <sub>1</sub> = 0.1511, <i>wR</i> <sub>2</sub> = 0.1175
largest diff. peak and hole [fm Å <sup>-3</sup> ]	1.070 and −0.978

atoms in this study; the phenyl carbon atoms did not merit special attention and, in any event, their displacement parameters are naturally constrained by the geometry of the ring.

The vertical detector axis is nearly parallel to the real-space direction [210]. The bonds of interest (H28B···F1, H35 A···F1) are approximately perpendicular to [210] and are thus least affected by the inherent paucity of data near the detector axis for only one mounting of the (triclinic) crystal in this instrument geometry. The same remark applies to the components of the thermal-displacement tensors and may lead to them becoming nonpositive definite. However, refinement of all the components of the tensors was still needed to correctly model the displacements in the horizontal plane. Other data collections on VIVALDI, for which monochromatic data for the same compound are also available, indicate that the bond distances from anisotropic refinements are more accurate than the values from isotropic refinements provided that the data permits sensible refinement of the horizontal plane components. These conclusions were borne out in a series of refinements in which various numbers of atoms were refined anisotropically; the H···F distances differed insignificantly and the estimated standard deviations were smaller than, for example, the C28–H28B bond which is more and nearly parallel to the vertical axis. The final structural refinement yielded *R*<sub>1</sub> = 0.0642 for 4132 $F_o$  > 4 $\sigma$ ( $F_o$ ) data, and *wR*<sub>2</sub> = 0.1175 and GOF = 1.117 for all data.

**X-ray crystallography:** For **5**: C<sub>39</sub>H<sub>41</sub>NOZr, *M*<sub>w</sub> = 630.98, monoclinic, *P*2<sub>1</sub>/*n*, *a* = 10.592(2), *b* = 21.642(4), *c* = 14.410(3) Å,  $\beta$  = 92.86(3)°, *V* = 3299.1(11) Å<sup>3</sup>, *Z* = 4,  $\rho_{\text{calcd}}$  = 1.270 g cm<sup>-3</sup>,  $\mu(\text{MoK}\alpha)$  = 0.363 mm<sup>-1</sup>, *F*(000) = 1320, *T* = 301(2) K,  $2\theta_{\text{max}}$  = 50.7°, 4725 independent reflections (*R*<sub>int</sub> = 0.0336), 379 variable parameters, *R*<sub>1</sub> = 0.036 [*I* > 2 $\sigma$ (*I*)], *wR*<sub>2</sub> = 0.083, GOF(*F*<sup>2</sup>) = 0.881, largest diff. peak/hole = 0.41/−0.40 e Å<sup>-3</sup>. For **7**: C<sub>36</sub>H<sub>13</sub>Cl<sub>2</sub>NO<sub>2</sub>Zr, *M*<sub>w</sub> = 683.87, monoclinic, *P*2<sub>1</sub>/*c*, *a* = 14.160(3), *b* = 12.883(3), *c* = 19.260(4) Å,  $\beta$  = 97.21(3)°, *V* = 3485.7(13) Å<sup>3</sup>, *Z* = 4,  $\rho_{\text{calcd}}$  = 1.303 g cm<sup>-3</sup>,  $\mu(\text{MoK}\alpha)$  = 0.499 mm<sup>-1</sup>, *F*(000) = 1424, *T* = 293(2) K,  $2\theta_{\text{max}}$  =

50.4°, 4573 independent reflections (*R*<sub>int</sub> = 0.0454), 376 variable parameters, *R*<sub>1</sub> = 0.047 [*I* > 2 $\sigma$ (*I*)], *wR*<sub>2</sub> = 0.121, GOF(*F*<sup>2</sup>) = 0.930, largest diff. peak/hole = 0.50/−0.30 e Å<sup>-3</sup>. For **9**: C<sub>41</sub>H<sub>39</sub>F<sub>6</sub>NOTi, *M*<sub>w</sub> = 723.66, monoclinic, *P*2<sub>1</sub>/*n*, *a* = 10.6069(3), *b* = 10.7982(3), *c* = 31.4667(8) Å,  $\beta$  = 94.7610(10)°, *V* = 3591.62(17) Å<sup>3</sup>, *Z* = 4,  $\rho_{\text{calcd}}$  = 1.338 g cm<sup>-3</sup>,  $\mu(\text{MoK}\alpha)$  = 0.303 mm<sup>-1</sup>, *F*(000) = 1504, *T* = 150(2) K,  $2\theta_{\text{max}}$  = 51°, 6676 independent reflections (*R*<sub>int</sub> = 0.0708), 452 variable parameters, *R*<sub>1</sub> = 0.065 [*I* > 2 $\sigma$ (*I*)], *wR*<sub>2</sub> = 0.166, GOF(*F*<sup>2</sup>) = 1.051, largest diff. peak/hole = 1.02/−1.06 e Å<sup>-3</sup>. For **10**: C<sub>40</sub>H<sub>39</sub>F<sub>4</sub>NOTi, *M*<sub>w</sub> = 673.64, monoclinic, *P*2<sub>1</sub>/*n*, *a* = 13.790(3), *b* = 15.478(3), *c* = 16.345(3) Å,  $\beta$  = 102.04(3)°, *V* = 3412.0(12) Å<sup>3</sup>, *Z* = 4,  $\rho_{\text{calcd}}$  = 1.311 g cm<sup>-3</sup>,  $\mu(\text{MoK}\alpha)$  = 0.305 mm<sup>-1</sup>, *F*(000) = 1408, *T* = 253(2) K,  $2\theta_{\text{max}}$  = 50.8°, 5825 independent reflections (*R*<sub>int</sub> = 0.0388), 424 variable parameters, *R*<sub>1</sub> = 0.041 [*I* > 2 $\sigma$ (*I*)], *wR*<sub>2</sub> = 0.116, GOF(*F*<sup>2</sup>) = 1.047, largest diff. peak/hole = 0.51/−0.30 e Å<sup>-3</sup>. For **12**: C<sub>40</sub>H<sub>39</sub>F<sub>4</sub>NOTi, *M*<sub>w</sub> = 673.64, orthorhombic, *P*2<sub>1</sub>2<sub>1</sub>2<sub>1</sub>, *a* = 10.182(2), *b* = 15.879(3), *c* = 21.376(4) Å, *V* = 3456.1(12) Å<sup>3</sup>, *Z* = 4,  $\rho_{\text{calcd}}$  = 1.295 g cm<sup>-3</sup>,  $\mu(\text{MoK}\alpha)$  = 0.301 mm<sup>-1</sup>, *F*(000) = 1408, *T* = 253(2) K,  $2\theta_{\text{max}}$  = 47.3°, 3056 independent reflections (*R*<sub>int</sub> = 0.0678), 206 variable parameters, *R*<sub>1</sub> = 0.066 [*I* > 2 $\sigma$ (*I*)], *wR*<sub>2</sub> = 0.162, GOF(*F*<sup>2</sup>) = 0.908, largest diff. peak/hole = 0.44/−0.38 e Å<sup>-3</sup>.

CCDC-281869 (**1**; neutron diffraction), CCDC-190343<sup>[21]</sup> (**4**), CCDC-281867 (**9**), and CCDC-280315–280318 (**7**, **5**, **12**, and **10**, respectively) contain the supplementary crystallographic data for this paper. These data can be obtained free of charge from the Cambridge Crystallographic Data Centre via [www.ccdc.cam.ac.uk/data\\_request/cif](http://www.ccdc.cam.ac.uk/data_request/cif).

**Polymerization procedures:** Ethylene polymerization was carried out under atmospheric pressure in toluene in a 500-mL glass reactor equipped with a propeller-like stirrer. Toluene (250 mL) was introduced into the nitrogen-purged reactor and stirred (600 rpm). The toluene was thermostated at 25°C, and the ethylene gas feed (100 Lh<sup>-1</sup>) was then started. After 15 min, polymerization was initiated by adding toluene solutions of the co-catalyst and then catalyst to the reactor whilst vigorously stirring (600 rpm) the mixture. After the prescribed time, isobutyl alcohol (10 mL) was added to terminate the polymerization and the ethylene gas feed was stopped. Methanol (1000 mL) and concentrated HCl (2 mL) were added to the resulting mixture. The polymer was collected by filtration, washed with methanol (200 mL), and dried in vacuo at 80°C for 10 h.

Ethylene/propylene copolymerization was performed by using a similar procedure to that for ethylene polymerization, except ethylene (100 Lh<sup>-1</sup>) and propylene (100 Lh<sup>-1</sup>) were used. After the prescribed time, isobutyl alcohol (10 mL) was added to terminate the polymerization and the olefin gas feed was stopped. Concentrated HCl (2 mL) was added to the resulting mixture and the mixture was washed with water (3 × 250 mL) and concentrated in vacuo. The resultant polymer was dried in vacuo at 130°C for 10 h.

Ethylene/NB copolymerization was performed using a similar procedure to that for ethylene polymerization, except the prescribed amount of NB (1 g) was added to the toluene before the ethylene gas feed (50 Lh<sup>-1</sup>) was started. The polymerization was quenched after the prescribed time by the addition of methanol (5 mL) and the ethylene gas feed was stopped. The resulting mixture was added to a stirred solution of acidic methanol (500 mL including 5 mL of conc. HCl) and acetone (500 mL). The polymer was collected by filtration, washed with methanol (3 × 200 mL), and dried in vacuo at 130°C for 10 h.

## Acknowledgements

M.C.W.C. is grateful to the Research Grants Council of the Hong Kong SAR, China [HKU 7095/00P], the City University of Hong Kong, and The University of Hong Kong for financial support, Dr. Haruyuki Makio for helpful discussions, Dr. Glenna S. M. Tong for assistance with DFT calculations, and Prof. Chi-Ming Che for supporting this work. J.M.C. wishes to thank the Royal Society for a University Research Fellowship, St. Catharine's College, Cambridge for a Senior Research Fellowship, the Institut Laue-Langevin, Grenoble, France for financial support and facility access during the commissioning of VIVALDI, and the University of

Durham for provision of X-ray diffraction facilities through a Long Term Visitor position.

- [1] a) Z. Dawoodi, M. L. H. Green, V. S. B. Mtetwa, K. Prout, *J. Chem. Soc., Chem. Commun.* **1982**, 1410–1411; b) M. Brookhart, M. L. H. Green, L. L. Wong, *Prog. Inorg. Chem.* **1988**, *36*, 1–124.
- [2] a) W. E. Piers, J. E. Bercaw, *J. Am. Chem. Soc.* **1990**, *112*, 9406–9407; b) R. H. Grubbs, G. W. Coates, *Acc. Chem. Res.* **1996**, *29*, 85–93; c) L. Resconi, L. Cavallo, A. Fait, F. Piemontes, *Chem. Rev.* **2000**, *100*, 1253–1345.
- [3] a) A. D. Horton, A. G. Orpen, *Organometallics* **1991**, *10*, 3910–3918; b) A. R. Siedle, R. A. Newmark, W. M. Lamanna, J. C. Huffman, *Organometallics* **1993**, *12*, 1491–1492; c) X. Yang, C. L. Stern, T. J. Marks, *J. Am. Chem. Soc.* **1994**, *116*, 10015–10031; d) E. Y. X. Chen, T. J. Marks, *Chem. Rev.* **2000**, *100*, 1391–1434.
- [4] a) J. Ruwwe, G. Erker, R. Fröhlich, *Angew. Chem.* **1996**, *108*, 108–110; *Angew. Chem. Int. Ed. Engl.* **1996**, *35*, 80–82; b) Y. Sun, R. E. v. H. Spence, W. E. Piers, M. Parvez, G. P. A. Yap, *J. Am. Chem. Soc.* **1997**, *119*, 5132–5143; c) J. Karl, G. Erker, R. Fröhlich, *J. Am. Chem. Soc.* **1997**, *119*, 11165–11173.
- [5] C. S. Slone, D. A. Weinberger, C. A. Mirkin, *Prog. Inorg. Chem.* **1999**, *48*, 233–350.
- [6] a) U. Siemeling, *Chem. Rev.* **2000**, *100*, 1495–1526; b) L. H. Gade, *Chem. Commun.* **2000**, 173–181; c) H. Butenschön, *Chem. Rev.* **2000**, *100*, 1527–1564; d) P. Jutzi, T. Redeker, *Eur. J. Inorg. Chem.* **1998**, 663–674.
- [7] H. H. Brintzinger, D. Fischer, R. Mülhaupt, B. Rieger, R. M. Waymouth, *Angew. Chem.* **1995**, *107*, 1255–1283; *Angew. Chem. Int. Ed. Engl.* **1995**, *34*, 1143–1170.
- [8] a) J. Saito, M. Mitani, J. Mohri, Y. Yoshida, S. Matsui, S. Ishii, S. Kojoh, N. Kashiwa, T. Fujita, *Angew. Chem.* **2001**, *113*, 3002–3004; *Angew. Chem. Int. Ed.* **2001**, *40*, 2918–2920; b) J. Saito, M. Mitani, M. Onda, J. Mohri, S. Ishii, Y. Toshiida, T. Nakano, H. Tanaka, T. Matsugi, S. Kojoh, N. Kashiwa, T. Fujita, *Macromol. Rapid Commun.* **2001**, *22*, 1072–1075; c) S. Ishii, J. Saito, M. Mitani, J. Mohri, N. Matsukawa, Y. Tohi, S. Matsui, N. Kashiwa, T. Fujita, *J. Mol. Catal. A* **2002**, *179*, 11–16; d) M. Mitani, R. Furuyama, J. Mohri, J. Saito, S. Ishii, H. Terao, N. Kashiwa, T. Fujita, *J. Am. Chem. Soc.* **2002**, *124*, 7888–7889; e) M. Mitani, J. Mohri, Y. Yoshida, J. Saito, S. Ishii, K. Tsuru, S. Matsui, R. Furuyama, T. Nakano, H. Tanaka, S. Kojoh, T. Matsugi, N. Kashiwa, T. Fujita, *J. Am. Chem. Soc.* **2002**, *124*, 3327–3336; f) M. Mitani, R. Furuyama, J. Mohri, J. Saito, S. Ishii, H. Terao, T. Nakano, H. Tanaka, T. Fujita, *J. Am. Chem. Soc.* **2003**, *125*, 4293–4305; g) S. Ishii, R. Furuyama, N. Matsukawa, J. Saito, M. Mitani, H. Tanaka, T. Fujita, *Macromol. Rapid Commun.* **2003**, *24*, 452–456; h) M. Mitani, T. Nakano, T. Fujita, *Chem. Eur. J.* **2003**, *9*, 2396–2403; i) M. Mitani, J. Saito, S. Ishii, Y. Nakayama, H. Makio, N. Matsukawa, S. Matsui, J. Mohri, R. Furuyama, H. Terao, H. Bando, H. Tanaka, T. Fujita, *Chem. Rec.* **2004**, *4*, 137–158; j) H. Makio, T. Fujita, *Bull. Chem. Soc. Jpn.* **2005**, *78*, 52–66; k) R. Furuyama, M. Mitani, J. Mohri, R. Mori, H. Tanaka, T. Fujita, *Macromolecules* **2005**, *38*, 1546–1552; l) R. Furuyama, J. Saito, S. Ishii, H. Makio, M. Mitani, H. Tanaka, T. Fujita, *J. Organomet. Chem.* **2005**, *690*, 4398–4413.
- [9] a) J. Tian, P. D. Hustad, G. W. Coates, *J. Am. Chem. Soc.* **2001**, *123*, 5134–5135; b) P. D. Hustad, J. Tian, G. W. Coates, *J. Am. Chem. Soc.* **2002**, *124*, 3614–3621; c) A. F. Mason, G. W. Coates, *J. Am. Chem. Soc.* **2004**, *126*, 16326–16327.
- [10] Regarding non-fluorinated steric effects upon living behavior, compare: a) S. Reinartz, A. F. Mason, E. B. Lobkovsky, G. W. Coates, *Organometallics* **2003**, *22*, 2542–2544; b) R. Furuyama, J. Saito, S. Ishii, M. Mitani, S. Matsui, Y. Tohi, H. Makio, N. Matsukawa, H. Tanaka, T. Fujita, *J. Mol. Catal. A* **2003**, *200*, 31–42.
- [11] a) G. Milano, L. Cavallo, G. Guerra, *J. Am. Chem. Soc.* **2002**, *124*, 13368–13369; b) G. Talarico, V. Busico, L. Cavallo, *J. Am. Chem. Soc.* **2003**, *125*, 7172–7173; c) G. Talarico, V. Busico, L. Cavallo, *Organometallics* **2004**, *23*, 5989–5993.
- [12] a) J. A. K. Howard, V. J. Hoy, D. O'Hagan, G. T. Smith, *Tetrahedron* **1996**, *52*, 12613–12622; b) J. D. Dunitz, R. Taylor, *Chem. Eur. J.* **1997**, *3*, 89–98; c) B. E. Smart, *J. Fluorine Chem.* **2001**, *109*, 3–11; d) G. R. Desiraju, *Acc. Chem. Res.* **2002**, *35*, 565–573; e) J. D. Dunitz, A. Gavazzotti, *Angew. Chem.* **2005**, *117*, 1796–1819; *Angew. Chem. Int. Ed.* **2005**, *44*, 1766–1787; f) K. Reichenbacher, H. I. Süß, J. Hulliger, *Chem. Soc. Rev.* **2005**, *34*, 22–30.
- [13] The value of 2.54 Å has been proposed (R. S. Rowland, R. Taylor, *J. Phys. Chem.* **1996**, *100*, 7384–7391), but the use of Pauling and Bondi radii give values of 2.55 and 2.67 Å, respectively.
- [14] a) V. A. Kumar, N. S. Begum, K. Venkatesan, *J. Chem. Soc., Perkin Trans. 2* **1993**, 463–467; b) L. Shimoni, H. L. Carrell, J. P. Glusker, M. M. Coombs, *J. Am. Chem. Soc.* **1994**, *116*, 8162–8168; c) H.-C. Weiss, R. Boese, H. L. Smith, M. M. Haley, *Chem. Commun.* **1997**, 2403–2404; d) D. J. Teff, J. C. Huffman, K. G. Caulton, *Inorg. Chem.* **1997**, *36*, 4372–4380; e) V. R. Thalladi, H.-C. Weiss, D. Bläser, R. Boese, A. Nangia, G. R. Desiraju, *J. Am. Chem. Soc.* **1998**, *120*, 8702–8710; f) P. A. Deck, M. J. Lane, J. L. Montgomery, C. Slebodnick, F. R. Fronczek, *Organometallics* **2000**, *19*, 1013–1024; g) U. Fekl, R. van Eldik, S. Lovell, K. I. Goldberg, *Organometallics* **2000**, *19*, 3535–3542; h) M. P. Thornberry, C. Slebodnick, P. A. Deck, F. R. Fronczek, *Organometallics* **2000**, *19*, 5352–5369; i) H. Lee, C. B. Knobler, M. F. Hawthorne, *Chem. Commun.* **2000**, 2485–2486; j) V. R. Vangala, A. Nangia, V. M. Lynch, *Chem. Commun.* **2002**, 1304–1305; k) A. J. Mountford, D. L. Hughes, S. J. Lancaster, *Chem. Commun.* **2003**, 2148–2149.
- [15] a) W. Caminati, S. Melandri, P. Moreschini, P. G. Favero, *Angew. Chem.* **1999**, *111*, 3105–3107; *Angew. Chem. Int. Ed.* **1999**, *38*, 2924–2925; b) W. Caminati, J. C. López, J. L. Alonso, J.-U. Grabow, *Angew. Chem.* **2005**, *117*, 3908–3912; *Angew. Chem. Int. Ed.* **2005**, *44*, 3840–3844.
- [16] a) I. Hyla-Kryspin, G. Haufe, S. Grimme, *Chem. Eur. J.* **2004**, *10*, 3411–3422; b) E. Kryachko, S. Scheiner, *J. Phys. Chem. A* **2004**, *108*, 2527–2535; c) X. Li, L. Liu, H. B. Schlegel, *J. Am. Chem. Soc.* **2002**, *124*, 9639–9647.
- [17] a) M. L. Renak, G. P. Bartholomew, S. Wang, P. J. Ricatto, R. J. Lachicotte, G. C. Bazan, *J. Am. Chem. Soc.* **1999**, *121*, 7787–7799; b) S. W. Watt, C. Dai, A. J. Scott, J. M. Burke, R. L. Thomas, J. C. Collings, C. Viney, W. Clegg, T. B. Marder, *Angew. Chem.* **2004**, *116*, 3123–3125; *Angew. Chem. Int. Ed.* **2004**, *43*, 3061–3063; c) C. E. Smith, P. S. Smith, R. L. Thomas, E. G. Robins, J. C. Collings, C. Dai, A. J. Scott, S. Borwick, A. S. Batsanov, S. W. Watt, A. J. Clark, C. Viney, J. A. K. Howard, W. Clegg, T. B. Marder, *J. Mater. Chem.* **2004**, *14*, 413–420.
- [18] a) C.-Y. Kim, J. S. Chang, J. B. Doyon, T. T. Baird, Jr., C. A. Fierke, A. Jain, D. W. Christianson, *J. Am. Chem. Soc.* **2000**, *122*, 12125–12134; b) J. Parsch, J. W. Engels, *J. Am. Chem. Soc.* **2002**, *124*, 5664–5672; c) J. W. Olsen, D. W. Banner, P. Seiler, U. O. Sander, A. D'Arcy, M. Stihle, K. Müller, F. Diederich, *Angew. Chem.* **2003**, *115*, 2611–2615; *Angew. Chem. Int. Ed.* **2003**, *42*, 2507–2511; d) J. S. Lai, J. Qu, E. T. Kool, *Angew. Chem.* **2003**, *115*, 6155–6159; *Angew. Chem. Int. Ed.* **2003**, *42*, 5973–5977; e) E. A. Meyer, R. K. Castellano, F. Diederich, *Angew. Chem.* **2003**, *115*, 1244–1287; *Angew. Chem. Int. Ed.* **2003**, *42*, 1210–1250.
- [19] a) S. M. Ngola, D. A. Dougherty, *J. Org. Chem.* **1998**, *63*, 4566–4567; b) W. Lu, M. C. W. Chan, N. Zhu, C. M. Che, Z. He, K. Y. Wong, *Chem. Eur. J.* **2003**, *9*, 6155–6166.
- [20] M. C. W. Chan, K. H. Tam, Y. L. Pui, N. Zhu, *J. Chem. Soc., Dalton Trans.* **2002**, 3085–3087.
- [21] S. C. F. Kui, N. Zhu, M. C. W. Chan, *Angew. Chem.* **2003**, *115*, 1666–1670; *Angew. Chem. Int. Ed.* **2003**, *42*, 1628–1632.
- [22] V. C. Gibson, S. K. Spitzmesser, *Chem. Rev.* **2003**, *103*, 283–315.
- [23] a) G. J. Pindado, M. Thornton-Pett, M. Bouwkamp, A. Meetsma, B. Hessen, M. Bochmann, *Angew. Chem.* **1997**, *109*, 2457–2460; *Angew. Chem. Int. Ed. Engl.* **1997**, *36*, 2358–2361; b) G. G. Lavoie, R. G. Bergman, *Angew. Chem.* **1997**, *109*, 2555–2558; *Angew. Chem. Int. Ed. Engl.* **1997**, *36*, 2450–2452; c) B. Ray, T. G. Neyroud, M. Kapon, Y. Eichen, M. S. Eisen, *Organometallics* **2001**, *20*, 3044–

- 3055; d) M. Said, M. Thornton-Pett, M. Bochmann, *J. Chem. Soc., Dalton Trans.* **2001**, 2844–2849.
- [24] M. Bouwkamp, D. van Leusen, A. Meetsma, B. Hessen, *Organometallics* **1998**, *17*, 3645–3647.
- [25] a) P. E. O'Connor, D. J. Morrison, S. Steeves, K. Burrage, D. J. Berg, *Organometallics* **2001**, *20*, 1153–1160; b) L. Lavanant, T.-Y. Chou, Y. Chi, C. W. Lehmann, L. Toupet, J. F. Carpentier, *Organometallics* **2004**, *23*, 5450.
- [26] I. J. Bruno, J. C. Cole, P. R. Edgington, M. Kessler, C. F. Macrae, P. McCabe, J. Pearson, R. Taylor, *Acta Crystallogr. Sect. B* **2002**, *58*, 389–397.
- [27] a) J. M. Cole, V. C. Gibson, J. A. K. Howard, G. J. McIntyre, G. L. P. Walker, *Chem. Commun.* **1998**, 1829–1830; b) R. Bau, S. A. Mason, B. O. Patrick, C. S. Adams, W. B. Sharp, P. Legzdins, *Organometallics* **2001**, *20*, 4492–4501; c) W. Baratta, C. Mealli, E. Herdtweck, A. Ienco, S. A. Mason, P. Rigo, *J. Am. Chem. Soc.* **2004**, *126*, 5549–5562.
- [28] a) T. Yoshida, N. Koga, K. Morokuma, *Organometallics* **1995**, *14*, 746–758; b) J. C. W. Lohrenz, T. K. Woo, T. Ziegler, *J. Am. Chem. Soc.* **1995**, *117*, 12794–12800.
- [29] H. Plenio, *Chem. Rev.* **1997**, *97*, 3363–3384.
- [30] E. Y. Tshuva, I. Goldberg, M. Kol, Z. Goldschmidt, *Organometallics* **2001**, *20*, 3017–3028.
- [31] a) H. Memmler, K. Walsh, L. H. Gade, J. W. Lauher, *Inorg. Chem.* **1995**, *34*, 4062–4068; b) B. Findeis, M. Schubart, L. H. Gade, F. Möller, I. Scowen, M. McPartlin, *J. Chem. Soc. Dalton Trans.* **1996**, 125–132.
- [32] a) M. Bochmann, S. J. Lancaster, *Organometallics* **1993**, *12*, 633–640; b) A. D. Horton, J. de With, A. J. van der Linden, H. van der Weg, *Organometallics* **1996**, *15*, 2672–2674; the use of high-field <sup>1</sup>H NMR resonances for *o*-Ph as a criterion is less reliable because the shifts can also be influenced by the ring currents of ancillary ligands: c) X. Bei, D. C. Swenson, R. F. Jordan, *Organometallics* **1997**, *16*, 3282–3302.
- [33] For examples, see: a) P. C. Myhre, J. W. Edmonds, J. D. Kruger, *J. Am. Chem. Soc.* **1966**, *88*, 2459–2466; b) R. E. Wasylshen, M. Barfield, *J. Am. Chem. Soc.* **1975**, *97*, 4545–4552; c) G. Yamamoto, M. Ôki, *J. Org. Chem.* **1984**, *49*, 1913–1917; d) A. Mele, B. Vergani, F. Viani, S. V. Leille, A. Farina, P. Bravo, *Eur. J. Org. Chem.* **1999**, 187–196; e) T. J. Barbarich, C. D. Rithner, S. M. Miller, O. P. Anderson, S. H. Strauss, *J. Am. Chem. Soc.* **1999**, *121*, 4280–4281.
- [34] Without access to the Amsterdam density functional (ADF) program employed by Fujita et al. for studying FI catalysts, we set out to verify that DFT calculations using the Gaussian program can give meaningful results that can be compared with those from the ADF program in the context of this work. Hence, we have shown that the calculated structure of [[1-(2,6-F<sub>2</sub>C<sub>6</sub>H<sub>3</sub>N=CH)-2-O-3-*t*BuC<sub>6</sub>H<sub>3</sub>]<sub>2</sub>TiCl<sub>2</sub>] closely resembles that predicted using ADF and the X-ray crystal structure, while good agreement was also observed between the calculated structure of **1** and the crystallographic determinations.
- [35] S. Matsui, M. Mitani, J. Saito, Y. Tohi, H. Makio, N. Matsukawa, Y. Takagi, K. Tsuru, M. Nitabaru, T. Nakano, H. Tanaka, N. Kashiwa, T. Fujita, *J. Am. Chem. Soc.* **2001**, *123*, 6847–6856.
- [36] For example, see: P. D. Knight, A. J. Clarke, B. S. Kimberley, R. A. Jackson, P. Scott, *Chem. Commun.* **2002**, 352–353.
- [37] Y. Yoshida, J. Mohri, S. Ishii, M. Mitani, J. Saito, S. Matsui, H. Makio, T. Nakano, H. Tanaka, M. Onda, Y. Yamamoto, A. Mizuno, T. Fujita, *J. Am. Chem. Soc.* **2004**, *126*, 12023–12032.
- [38] H. Makio, T. Fujita, *Macromol. Symp.* **2004**, *213*, 221–233.
- [39] R. R. Schrock, P. J. Bonitatebus, Jr., Y. Schrodi, *Organometallics* **2001**, *20*, 1056–1058.
- [40] R. R. Schrock, J. Adamchuk, K. Ruhland, L. P. H. Lopez, *Organometallics* **2003**, *22*, 5079–5091.
- [41] Application of an abrupt cut-off distance should be treated with caution because the electrostatic nature of an intramolecular interaction as a function of increasing separation (*r*) exhibits 1/*r*<sup>*n*</sup> dependence, and hence the progressive weakening of this interaction is continuous.
- [42] U. Zucchini, E. Albizzati, U. Giannini, *J. Organomet. Chem.* **1971**, *26*, 357–372.
- [43] J. H. Wengrovius, R. R. Schrock, *J. Organomet. Chem.* **1981**, *205*, 319–327.
- [44] A. M. S. Silva, L. M. P. M. Almeida, J. A. S. Cavaleiro, C. Foces-Foces, A. L. Llamas-Saiz, C. Fontenas, N. Jagerovic, J. Elguero, *Tetrahedron* **1997**, *53*, 11 645–11 658.
- [45] C. Dietrich-Buchecker, J. P. Sauvage, *Tetrahedron* **1990**, *46*, 503–512.
- [46] C. Wilkinson, J. A. Cowan, D. A. A. Myles, F. Cipriani, G. J. McIntyre, *Neutron News* **2002**, *13*, 37–41.
- [47] a) J. W. Campbell, *J. Appl. Crystallogr.* **1995**, *28*, 228–236; b) J. W. Campbell, Q. Hao, M. M. Harding, N. D. Nguti, C. Wilkinson, *J. Appl. Crystallogr.* **1998**, *31*, 23–31.
- [48] C. Wilkinson, H. W. Khamis, R. F. D. Stansfield, G. J. McIntyre, *J. Appl. Crystallogr.* **1988**, *21*, 471–478.
- [49] J. W. Campbell, J. Habash, J. R. Helliwell, K. Moffat, *Inf. Quart. Protein Crystallogr.* **1986**, *18*, 23–31.
- [50] SHELXL-97, Program for the Refinement of Crystal Structures, G. M. Sheldrick, University of Göttingen, Göttingen (Germany), **1997**.

Received: August 28, 2005

Published online: December 19, 2005